AD-A063 954 SCIENCE APPLICATIONS INC MCLEAN VA F/G 18/8
X-RAY DOSE ENHANCEMENT, II.(U)
NOV 78 W L CHADSEY F19628-77-C-0181
UNCLASSIFIED SAI-102-78-011 RADC-TR-78-249 NL

1 OF 1
AD A063954

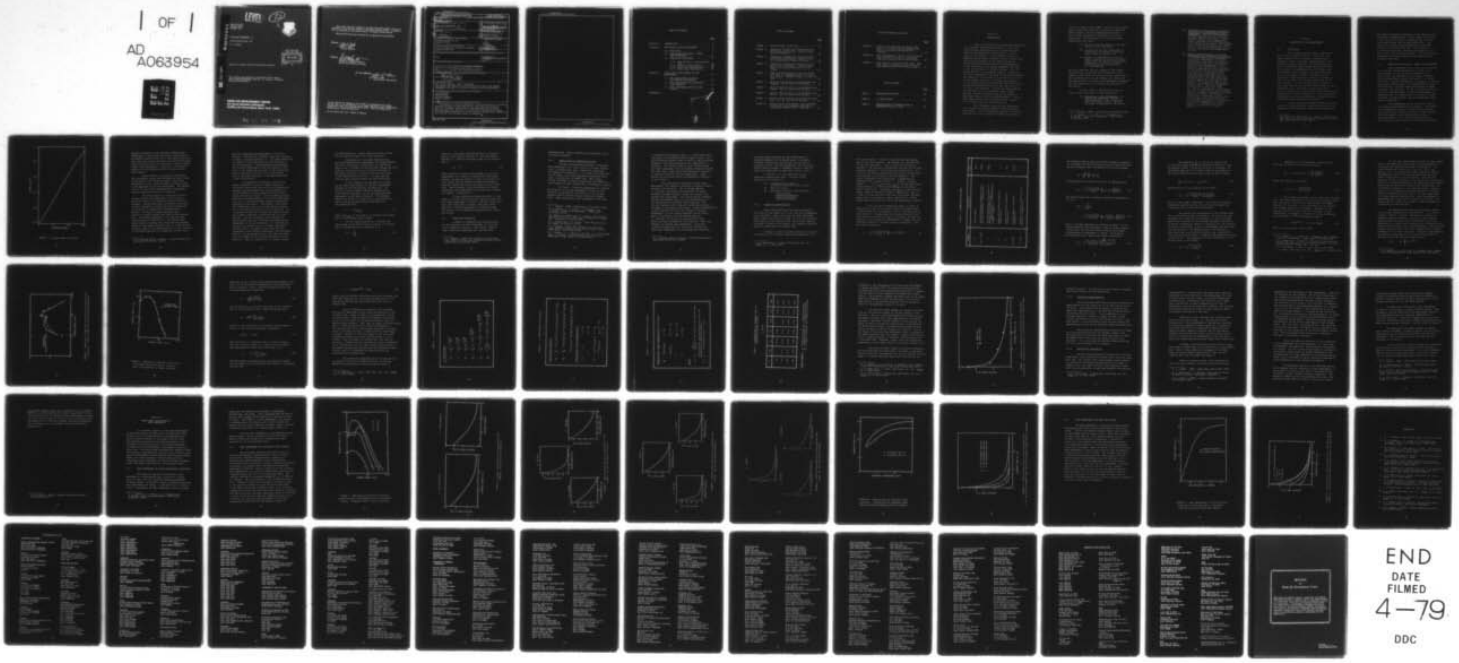

END
DATE FILMED
4-79
DDC

RADC-TR-78-249
Interim Report
November 1978

X-RAY DOSE ENHANCEMENT, II

Science Applications, Inc.

W. L. Chadsey

This research was supported by the Defense Nuclear Agency under Subtask Z99QAXTA040, Work Unit 71, entitled, "Secondary Electron Phenomenology".

ROME AIR DEVELOPMENT CENTER
Air Force Systems Command
Griffiss Air Force Base, New York 13441

This report has been reviewed by the RADC Information Office (OI) and is releasable to the National Technical Information Service (NTIS). At NTIS it will be releasable to the general public, including foreign nations.

RADC-TR-78-249 has been reviewed and is approved for publication.

APPROVED: John C. Garth
JOHN C. GARTH
Project Engineer

APPROVED: Robert M. Barrett
ROBERT M. BARRETT, Director
Solid State Sciences Division

FOR THE COMMANDER: John P. Huss
JOHN P. HUSS
Acting Chief, Plans Office

If your address has changed or if you wish to be removed from the RADC mailing list, or if the addressee is no longer employed by your organization, please notify RADC (ESR) Hanscom AFB MA 01731. This will assist us in maintaining a current mailing list.

Do not return this copy. Retain or destroy.

UNCLASSIFIED

SECURITY CLASSIFICATION OF THIS PAGE *(When Data Entered)*

REPORT DOCUMENTATION PAGE	READ INSTRUCTIONS BEFORE COMPLETING FORM
1. REPORT NUMBER: RADC-TR-78-249	2. GOVT ACCESSION NO. / 3. RECIPIENT'S CATALOG NUMBER
4. TITLE *(and Subtitle)*: X-RAY DOSE ENHANCEMENT, II	5. TYPE OF REPORT & PERIOD COVERED: Interim Report, No. 1
	6. PERFORMING ORG. REPORT NUMBER: SAI-102-78-011
7. AUTHOR(s): W. L. Chadsey	8. CONTRACT OR GRANT NUMBER(s): F19628-77-C-0181
9. PERFORMING ORGANIZATION NAME AND ADDRESS: Science Applications, Inc., McLean VA 22010	10. PROGRAM ELEMENT, PROJECT, TASK AREA & WORK UNIT NUMBERS: 62704H, CDNA0027
11. CONTROLLING OFFICE NAME AND ADDRESS: Deputy for Electronic Technology (RADC/ESR), Hanscom AFB MA 01731	12. REPORT DATE: November 1978
	13. NUMBER OF PAGES: 66 p.
14. MONITORING AGENCY NAME & ADDRESS *(if different from Controlling Office)*: Same	15. SECURITY CLASS. *(of this report)*: UNCLASSIFIED
	15a. DECLASSIFICATION/DOWNGRADING SCHEDULE: N/A

16. DISTRIBUTION STATEMENT *(of this Report)*

Approved for public release; distribution unlimited.

CDNA, Z99QAXT

17. DISTRIBUTION STATEMENT *(of the abstract entered in Block 20, if different from Report)*

Same — A040.00

18. SUPPLEMENTARY NOTES

RADC Project Engineer: John C. Garth (ESR)
This research was supported by the Defense Nuclear Agency under Subtask Z99QAXTA040, Work Unit 71, entitled, "Secondary Electron Phenomenology".

19. KEY WORDS *(Continue on reverse side if necessary and identify by block number)*

Dose Enhancement
Radiation Dose
Electron Transport
Radiation Effects

20. ABSTRACT *(Continue on reverse side if necessary and identify by block number)*

A discussion of x-ray dose enhancement at material interfaces is presented including definition, problem identification and worst-case estimation, prediction techniques, and analysis of dose enhancement characteristics. Empirical, analytical, and Monte Carlo prediction techniques are discussed. Dose enhancement calculations for various interface configurations, continuous x-ray sources, and thin high-Z layers are presented.

DD FORM 1 JAN 73 1473

UNCLASSIFIED

SECURITY CLASSIFICATION OF THIS PAGE *(When Data Entered)*

TABLE OF CONTENTS

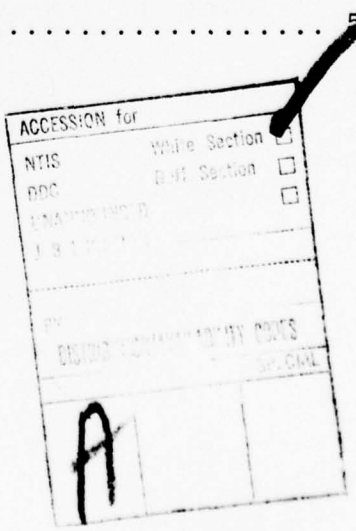

LIST OF FIGURES

LIST OF FIGURES (Continued)

LIST OF TABLES

Section 1

INTRODUCTION

Near an interface between dissimilar materials of a structure irradiated by x-rays or γ-rays, the local absorbed radiation dose in a material differs from the equilibrium dose which occurs in a bulk region of the material. The difference in dose is produced through energy transport by the electron flux driven in the materials by the photon radiation. The nonequilibrium dose occurs in the neighborhood of the interface, in the region bounded by the range of the most energetic of these electrons. For low energy photons, in the spectral range of several keV to several hundred keV, the depth of the nonequilibrium dose region is on the order to 1 to 100 μm in a low-Z (atomic number) material. For high energy photons in the spectral range of several MeV, the depth of the nonequilibrium dose region is on the order of 0.1 to 1 cm in a low-Z material. For the low energy photons, the peak dose in a low-Z material near a high-Z material interface can be as much as two orders of magnitude greater than the equilibrium dose. For the high energy photons, the peak dose can be a factor of two greater than the equilibrium dose.

This phenomenon, known as dose enhancement, is of concern in nuclear radiation effects analysis and testing. It is of particular concern in transient radiation effects in electronics (TRE) and radiation

effects in cables (cable SGEMP). Over the past several years we have been involved in research to obtain an understanding of the dose enhancement phenomenon and to develop methods for the prediction of dose enhancement. The main objectives of this research program have been three:

(1) develop a rigorous model for the calculation of dose enhancement,

(2) characterize the dose enhancement at low-Z/high-Z interfaces over a broad range of photon energies, and

(3) support the development of a user's guide to provide the radiation effects analyst with the means to predict dose enhancement for arbitrary material configuration and arbitrary x-ray or γ-ray spectrum.

The first objective was met through the development, documentation, and release of the POEM Monte Carlo computer code for the calculation of dose enhancement.[1] The second objective was met through the compilation and publication of the x-ray dose enhancement handbook.[2] The third objective is met through the publication of this report.

In this report we provide three types of input to the User's Guide to Dose Enhancement:

(1) Definition of dose enhancement. We address the questions: Why does dose enhancement occur? Under what conditions does it occur? What is the order of magnitude of the effect?

---

[1] W. L. Chadsey, "POEM," AFCRL Report TR-75-3034 (1975).

[2] W. L. Chadsey, J. C. Garth, R. L. Sheppard, and R. Murphy, "X-Ray Dose Enhancement," RADC Report TR-76-159 (1976).

(2) Description of the analysis techniques available to the prediction of dose enhancement. The techniques discussed include a prescription for obtaining an upper bound on the effect, a semi-empirical method for estimating the effect, and Monte Carlo computer codes for calculating the effect. This description includes discussion of the limitations of the various techniques and the relative advantages and disadvantages of each.

(3) Further characterization of the dose enhancement near high-Z/low-Z interfaces. (a) The previously published report, "X-Ray Dose Enhancement,"[2] provided description of the dose enhancement in silicon near gold and in polyethylene near gold for monochromatic x-ray sources in the range 10 keV to 2 MeV. Herein we describe the dose enhancement in silicon near gold for continuous x-ray spectra, in particular, for filtered, black body x-ray spectra, with temperatures ranging from 2 keV through 15 keV. (b) The calculations of dose enhancement published in the previous report were for "thick" gold layers, i.e. thicker than the maximum electron range. Herein we report calculations for thin gold layers. (c) The dose enhancement is calculated for several additional interface configurations, including aluminum/polyethylene, copper polyethylene, and silver/polyethylene, which when combined with the previously reported results for gold/polyethylene provide a good description of dose enhancement in a low-Z material as function of the atomic number of the interfacing high-Z material.

Section 2

PREDICTION OF DOSE ENHANCEMENT

2.1 DEFINITION

Dose is defined as the energy imparted to matter per unit mass of matter. X-rays and γ-rays impart energy to matter primarily through energy transfer to swift electrons – photoelectrons, Auger electrons, Compton electrons, and electron/positron pairs – which then impart energy through collisions. In a region of a homogeneous material farther from any boundary than the range of the most penetrating of these electrons, electron equilibrium occurs: the energy transported into a region by electrons is equal in the mean to the energy transported out by the electrons. In this case the dose is equal to the energy per unit mass locally removed from the photon radiation field – the kerma or equilibrium dose. Given the description of the photon fluence and spectrum, prediction of the equilibrium dose is straightforward using readily available tabulations or formulations of the photon energy absorbtion coefficient.[3]

Near an interface between dissimilar materials, or near a vacuum interface, electron equilibrium fails because of the differences in the electron production

---

[3] For example, E. Storm and H. I. Israel, "Photon Cross Sections from 0.001 to 100 MeV for Elements 1 through 100," LASL Report LA-3753 (1967).

and electron transport properties of the adjacent media: the energy transported into a local region by electrons is not equal to the energy transported out; thus the local dose differs from the equilibrium dose. The region of electron disequilibrium near an interface is known as the transition zone. The prediction of the dose within the transition zone requires treatment of the local electron transport. In the following paragraphs we discuss techniques for predicting the transition zone dose.

2.2 PROBLEM IDENTIFICATION - WORST CASE ESTIMATION

Dose enhancement occurs in the region adjacent to a material interface bounded by the range of the most energetic of the electrons liberated by the photon flux. The maximum electron energy is bounded by the maximum photon energy; the width of the transition zone is therefore bounded by the range of an electron with kinetic energy equal to the maximum photon energy. (For reference, electron range versus energy is shown in Figure 1 for silicon.) If one is concerned with the effects of radiation dose, or with the measurement of radiation dose, in a region which lies within a transition zone, as thus defined, the dose enhancement effect must be considered.

Dose enhancement arises through the failure of electron equilibrium near an interface. Equilibrium fails through two effects: electron emission across the interface and electron reflection at the interface. Electron emission across the interface produces dose enhancement if the electron emission yield of one material differs from that of the adjacent material.

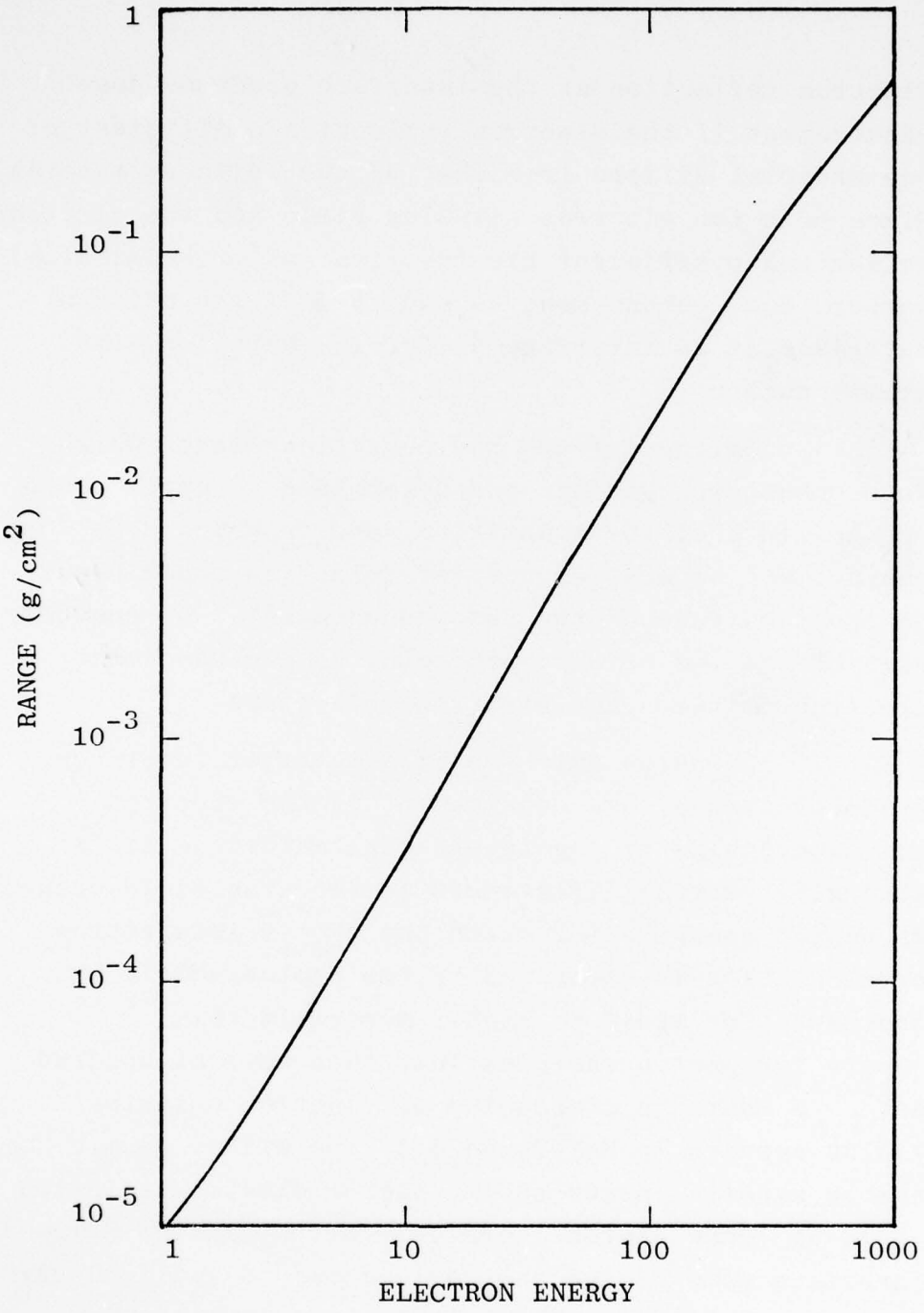

FIGURE 1. Electron Range in Silicon.

Electron reflection at the interface produces dose enhancement if the electron reflection coefficient of one material differs from that of the adjacent material. Since both the electron emission yield and the electron reflection coefficient are functions of material atomic number, dose enhancement is expected if the adjacent materials at an interface differ in characteristic atomic number.

Having defined the conditions under which dose enhancement occurs and determined an upper bound on the width of the transition zone in which dose enhancement occurs, we now determine the upper bound on the magnitude of the dose enhancement. We consider each of the two effects producing dose enhancement: electron emission and electron reflection.

Electron emission at a material interface produces strong dose enhancement if the electron emission yields of the interfacing materials differ strongly. Strong differences in electron yield occur at photon energies for which the photon interaction cross section is dominated by the photoelectric process. For mid-Z to high-Z materials this occurs for photon energies less then several hundred keV. (A thorough compendium of electrom emission yields appears in Reference 4.) The higher atomic number material produces the higher electron emission yield at these photon energies; thus at a high-Z/low-Z interface some of the energy imparted to swift electrons in the high-Z material is transported into the low-Z

---

[4] W. L. Chadsey and C. W. Wilson, "X-Ray Photoemission," HDL Report CR-75-138-1 (1975).

material producing dose enhancement in the low-Z material. The electron transport across the interface is thus an averaging process, i.e. the energy deposition is reduced in the high-Z material and increased in the low-Z material. A maximum upper bound estimate for the dose enhancement in the low-Z material (the ratio of the transition zone dose to the equilibrium dose) is therefore the ratio of the equilibrium dose in the high-Z material to the equilibrium dose in the low-Z material.

At higher photon energies, greater than several hundred keV in mid to high-Z materials, the photon interaction cross section is dominated by Compton electron production so that differences in electron emission yields between different atomic number materials are small. Electron emission across a material interface produces little dose enhancement; the ratio of equilibrium doses between interfacing materials is near unity. Nevertheless, significant dose enhancement can occur at these photon energies due to the electron reflection at the interface. At a high-Z/low-Z material interface the high-Z material has a higher reflection coefficient than the low-Z material, such that electrons are preferentially backscattered into the low-Z material producing dose enhancement in the low-Z material. At these photon energies the electron flux is strongly directed in the direction of the photon flux; since the dose enhancement occurs through backscatter from the high-Z material, the enhancement occurs only when the photon flux is incident on the interface through the low-Z material. (When the photon flux is incident through

the high-Z material, a small reduction in dose occurs in the transition zone of the low-Z material.)

Determination of an upper bound electron reflection-produced dose enhancement is straightforward. The worst case would be obtained for the conditions: photon flux is incident on the interface through the low-Z material; the electron flux is entirely directed in the photon direction, and the reflection coefficient of the high-Z material is unity. In such case the interface dose would be double the equilibrium dose.

We now summarize the procedure for obtaining an upper bound estimate of the dose enhancement. Consider an interface between two materials. Let material 1 be the higher-Z material and material 2 be the lower-Z material. We are concerned with dose enhancement in the lower-Z material. To determine whether the region of concern lies in the transition zone we obtain an upper bound on the width w of the transition zone:

$$w < r_e(h\nu_{max}) \tag{1}$$

where $r_e(h\nu_{max})$ is the range of an electron with energy equal to the maximum photon energy.

For low energy photons ($h\nu \lesssim 500$ keV) the upper bound on the relative dose D_r (ratio of interface dose to equilibrium dose in material 2) is

$$D_r < \frac{K_1}{K_2} \tag{2}$$

where K_1 is the kerma (equilibrium dose) in material 1 and K_2 is the kerma in material 2. For high energy photons ($h\nu > 500$ keV) the upper bound on the relative dose is

$$D_r < 2 \qquad (3)$$

(When obtaining an upper bound estimate for the dose enhancement in a structure irradiated by high energy photons, one must be careful to take into account the lower energy photons produced through scattering in materials positioned between the source and the interface. The low energy, scattered photons can produce significant dose enhancement at the interface as shown, for example, in Reference 5.)

If this bounding procedure indicates (1) the region of concern lies within the transition zone, and (2) a dose enhancement as great as the upper bound estimate would constitute a problem, then more careful analysis of the dose enhancement is required using one or more of the techniques discussed in the following section.

2.3 PREDICTION TECHNIQUES

A number of techniques have been developed for the prediction of dose enhancement at x-ray and γ-ray irradiated interfaces: Monte Carlo computer codes, analytical approximations, and empirical

---

[5] W. L. Chadsey, "Monte Carlo Analysis of X-Ray and γ-Ray Transition Zone Dose and Photo-Compton Current," "AFCRL Report TR-73-0572 (1973).

approximations. These techniques are discussed in the following paragraphs.

2.3.1. Compilations of Computational Data

The most straightforward method of predicting dose enhancement is to refer to one of several compilations of computational data. These data, appearing for example in references 2, 4, 5, and 6 and in Section 3 of this report, have been calculated using Monte Carlo codes, in particular the POEM[1] code. While there is high confidence in these calculations, the number of cases treated in these compilations is necessarily limited.

The report, "X-Ray Dose Enhancement,[2]" presents calculations of the dose enhancement in silicon near gold and in polyethylene near gold for a set of monochromatic photon spectra ranging from 10 keV through 2 MeV. These calculations were performed for the case

---

[1] W. L. Chadsey, "POEM," AFCRL Report TR-75-3034 (1975).

[2] W. L. Chadsey, J. C. Garth, R. L. Sheppard, and R. Murphy, "X-Ray Dose Enhancement," RADC Report TR-76-159 (1976).

[3] For example, E. Storm and H. I. Israel, "Photon Cross Sections from 0.001 to 100 MeV for Elements 1 through 100," LASL Report LA-3753 (1967).

[4] W. L. Chadsey and C. W. Wilson, "X-Ray Photoemission," HDL Report CR-75-138-1 (1975).

[5] W. L. Chadsey, "Monte Carlo Analysis of X-Ray and γ-Ray Transition Zone Dose and Photo-Compton Current," AFCRL Report TR-73-0572 (1973).

[6] W. L. Chadsey, B. L. Beers, V. W. Pine, D. J. Strickland and C. W. Wilson, "X-Ray Photoemission; X-Ray Dose Enhancement" RADC Report TR-77-253 (1977).

of equilibrium thickness of gold, i.e. gold layer thickness equal to the maximum electron range in gold. For gold thicknesses greater than or equal to the equilibrium thickness, the results presented are independent of thickness. For thinner layers of gold, which produce less dose enhancement (the equilibrium thickness provides the worst case), Monte Carlo calculations are required to accurately predict the dose enhancement. (Some results for thin gold layers are presented in Section 3 of this report.)

The calculations presented in "X-Ray Dose Enhancement" are limited to the case of photon incidence normal to the interface. For low energy photons, $h\nu \lesssim 400$ keV, the results are presented for normal incidence through the gold – which case produces the maximum dose enhancement. For oblique photon incidence, the dose enhancement scales to good approximation as the vacuum electron emission yield from gold. (The electron emission yield from gold versus photon angle of incidence is presented in the report, "X-Ray Photoemission;"[4] as shown therein the yield, and therefore the dose enhancement, are only weakly dependent on the photon angle of incidence.) For high photon energies, $h\nu \gtrsim 400$ keV, the results are presented for both photon incidence through the low-Z material, which case produces the maximum dose enhancement, and photon incidence through the gold, which case produces the least dose enhancement (or the maximum dose reduction.)

---

[4] W. L. Chadsey and C. W. Wilson, "X-Ray Photoemission," HDL Report CR-75-138-1 (1975).

For these photon energies the dose enhancement is strongly dependent on the photon angle of incidence; therefore, Monte Carlo calculations are required to accurately predict the dose enhancement for the case of oblique photon incidence. (Remember, however, that the worst-case enhancement is less than a factor of two.)

In Section 3 of this report we present additional computational data. Included in this compilation are results for

- continuous photon spectra (filtered, black body x-ray spectra)
- thin gold layers
- additional interface configurations —
  - copper/silicon
  - aluminum/polyethylene
  - copper/polyethylene
  - silver/polyethylene

2.3.2 Empirical Approximation

Burke and Garth[7] have developed an empirical algorithm for the prediction of the x-ray dose enhancement at an interface. Herein we review the Burke and Garth model, modify the model to include the electron reflection contribution to the interface dose, and further simplify the model to obtain a very simple, but reasonably accurate model for predicting the interface dose.

Consider a planar interface between two materials: let material 1 be the high-Z material and material 2 be

---

[7] E. A. Burke and J. C. Garth, IEEE Trans. Nuc. Sci., NS-23, No. 6, 1838 (1976).

the low-Z material. We want to predict the dose enhancement in the low-Z material. We consider two contributions to the dose enhancement: that by electrons arising in material 1 (the emission contribution) and that by electrons arising in material 2 (the reflection contribution). Let $\mu_i(h\nu)$ be the photon interaction cross section in material 1 for producing n_i electrons of initial energy E_i. The index i represents the interactions: K-photoelectric, L-photoelectric, M-photoelectric,..., K-Auger, L-Auger, M-Auger,... . Let $\mu_{en1}(h\nu)$ and $\mu_{en2}(h\nu)$ be the equilibrium energy absorption cross-sections (kerma) in materials 1 and 2, respectively. Let $R_1(E_i)$ and $R_2(E_i)$ be the electron ranges (csda) in materials 1 and 2, respectively; and let β_1 and β_2 be the electron reflection coefficients (diffuse backscatter) in materials 1 and 2, respectively. These symbol definitions and their units are summarized in Table 1.

We follow the development by Burke to obtain an expression for the relative dose (ratio of interface dose to equilibrium dose) in material 2 due to electron emission from material 1. Assume that the electron fluence in the bulk regions of materials 1 and 2 is isotropic and that the reflection coefficients are independent of energy; then the interface fluence of electrons arising in material 1, per unit photon fluence is

$$\phi_1 = \frac{1}{2} \frac{(1-\beta_1)(1+\beta_2)}{1-\beta_1\beta_2} \sum_i n_i \mu_i(h\nu) R_1(E_i) \qquad (4)$$

TABLE 1. PARAMETER DEFINITIONS

SYMBOL	DEFINITION	UNITS
$h\nu$	photon energy	keV
μ_{en1} (μ_{en2})	equilibrium energy absorption cross section in material 1 (material 2)	cm^2/g
μ_i	electron production cross section in material 1 for interaction i: i = K-photoelectric, L-photoelectric,... K-Auger, L-Auger,...	cm^2/g
n_i	number of electrons produced in interaction i	——
E_i	energy of electron produced in interaction i	keV
R_1 (R_2)	electron range in material 1 (material 2)	g/cm^2
β_1 (β_2)	electron reflection coefficient in material 1 (material 2)	——

The interface dose D_1 due to electrons arising in material 1 is the product of the differential electron fluence and the electron stopping power, integrated over electron energy

$$D_1 = \int \frac{d\phi_1}{dE} S_2(E)dE \tag{5}$$

Using equations (4) and (5) we obtain the approximation

$$D_1 = \frac{1}{2} \frac{(1-\beta_1)(1+\beta_2)}{1-\beta_1\beta_2} \sum_i n_i \mu_i(h\nu) \frac{R_1(E_i)}{R_2(E_i)} E_i \tag{6}$$

The relative dose due to electron emission from material 1 is then

$$D_{r1} = \frac{D_1}{\mu_{en2} h\nu}$$

$$= \frac{1}{2} \frac{(1-\beta_1)(1+\beta_2)}{(1-\beta_1\beta_2)} \sum_i n_i \frac{\mu_i(h\nu)}{\mu_{en2}(h\nu)} \frac{R_1(E_i)}{R_2(E_i)} \frac{E_i}{h\nu} \tag{7}$$

This is the same expression as obtained by Burke. We now further simplify this expression. Over the energy range of concern here, the ratio of electron ranges $R_1(E_i)/R_2(E_i)$ is approximately independent of energy. Let R_1/R_2 be the effective ratio; then we may rewrite equation (7):

$$D_{r1} = \frac{1}{2} \frac{(1-\beta_1)(1+\beta_2)}{(1-\beta_1\beta_2)} \frac{R_1}{R_2} \frac{\sum_i n_i \mu_i(h\nu) E_i}{\mu_{en2}(h\nu) h\nu} \tag{8}$$

The expression $\sum_i n_i \mu_i(h\nu) E_i$ in equation (8) is the total energy imparted to electrons in material 1 per unit photon fluence. By definition this is the kerma, the equilibrium dose per unit fluence, which is the product of the energy absorption cross section and the photon energy

$$\sum_i n_i \mu_i(h\nu) E_i = \mu_{en1}(h\nu) h\nu \tag{10}$$

Substituting (10) into equation (9) we obtain

$$D_{r1} = \frac{1}{2} \frac{(1-\beta_1)(1+\beta_2)}{1-\beta_1\beta_2} \frac{R_1}{R_2} \frac{\mu_{en1}(h\nu)}{\mu_{en2}(h\nu)} \tag{11}$$

This is a very simple expression: the ratio of the equilibrium doses modified by the ratio of electron ranges and a function of the reflection coefficients.

Now consider the contribution to the interface dose due to electrons arising in material 2. We follow the same procedure as in equations (4) through (11), but for energy deposition in material 2 for electrons arising in material 2. We obtain an expression similar to equation (11), but with the reflection coefficients β_1 and β_2 interchanged (the electrons are starting out on the opposite side of the interface) and with R_1 and μ_{en1} replaced by R_2 and μ_{en2}, respectively (the electrons are starting in material 2 and depositing energy in material 2). The expression for this contribution to the relative dose is thus simply

$$D_{r2} = \frac{1}{2} \frac{(1+\beta_1)(1-\beta_2)}{1-\beta_1\beta_2} \tag{12}$$

Summing the two contributions, equations (10) and (11), we obtain the total relative dose

$$D_r = f(\beta_2,\beta_1)+f(\beta_1,\beta_2)\frac{R_1}{R_2}\frac{\mu_{en1}(h\nu)}{\mu_{en2}(h\nu)} \quad (13)$$

where the function f is defined

$$f(\beta_1,\beta_2) = \frac{(1-\beta_1)(1+\beta_2)}{2(1-\beta_1\beta_2)} \quad (14)$$

For evaluating equation (13) to obtain the interface dose, the energy absorption cross sections are readily obtainable from photon cross section computations, for example, reference 2. The ratio of electron ranges can be obtained from a range tabulation, for example, reference 8. The electron reflection coefficients are available in data compilations, for example, reference 9, or can be obtained by using Burke's fit[10] to Darlington's data:[9]

$$\beta = 0.475Z^{0.177} - 0.40, \text{ for } 4 \le Z \le 92 \quad (15)$$

where Z is the material atomic number.

---

[2] W. L. Chadsey, J. C. Garth, R. L. Sheppard, and R. Murphy, "X-Ray Dose Enhancement," RADC Report TR-76-159 (1976).

[8] M. J. Berger and S. M. Seltzer, "Studies in Penetration of Charged Particles in Matter," National Academy of Sciences - National Research Council Publ. No. 1133.

[9] E. H. Darlington, J. Phys. D: Appl. Phys. 8, 85 (1975).

[10] E. A. Burke, IEEE Trans. Nuc. Sci., NS-24, No. 6, 2505 (1977).

To test this simple empirical model we made comparisons to the POEM code calculations of dose enhancement at a gold/silicon interface published in reference 2. For these comparisons we used $\beta_{Au} = 0.50$, $\beta_{Si} = 0.18$, and $R_{Au}/R_{Si} = 2.0$. We obtained the results shown in Figure 2. The agreement between the empirical model and the Monte Carlo calculations is quite reasonable: above 100 keV and below 20 keV the agreement is to within 20%, approximately within the standard deviation of the Monte Carlo calculation; between 20 keV and 100 keV there is some disagreement, but the maximum discrepancy is less than 50 percent. Shown in Figure 3 is a comparison of the predictions of the simple model with POEM code calculations of the dose enhancement at a copper/polyethylene interface. Here the agreement is remarkably good, everywhere to within a few percent. This simple empirical model, we conclude, is quite adequate for estimating the interface dose.

The empirical model thus far developed predicts only the dose immediately at the interface. It is also of interest, however, to predict the dose as a function of distance from the interface. This can be done with the empirical model provided that an additional simplifying approximation is made, that the dose profile produced by each of the electron source types (K-photoelectron, L-photoelectron, K-Auger electron, and so on) can be represented by a simple exponential of the form $a\exp(-bx)$. Using this approximation we obtain an expression for the relative dose profile in material 2 near the interface with material 1

$$D_r(x) = D_{ro} \sum_i a_i e^{-b_i x} \qquad (16)$$

---

[2] W. L. Chadsey, J. C. Garth, R. L. Sheppard, and R. Murphy, "X-Ray Dose Enhancement," RADC Report TR-76-159 (1976).

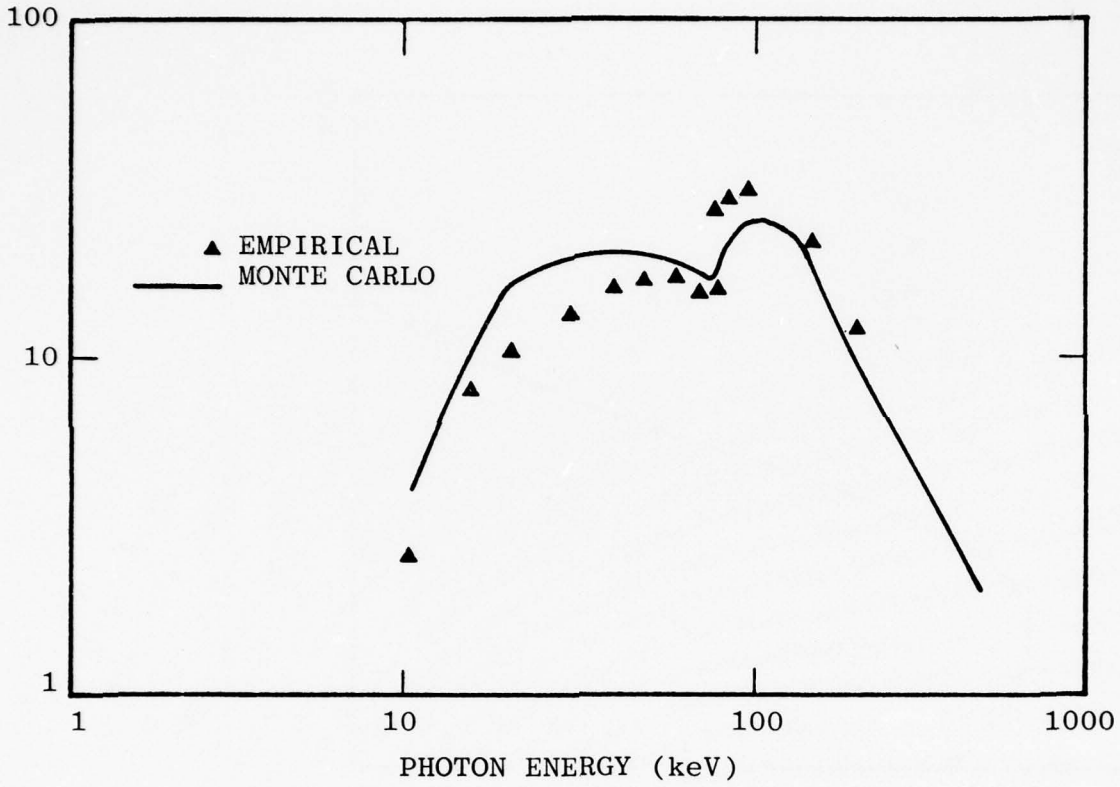

FIGURE 2. Comparison of Empirical Calculation with Monte Carlo Calculation: Relative Dose in Silicon at Gold Interface.

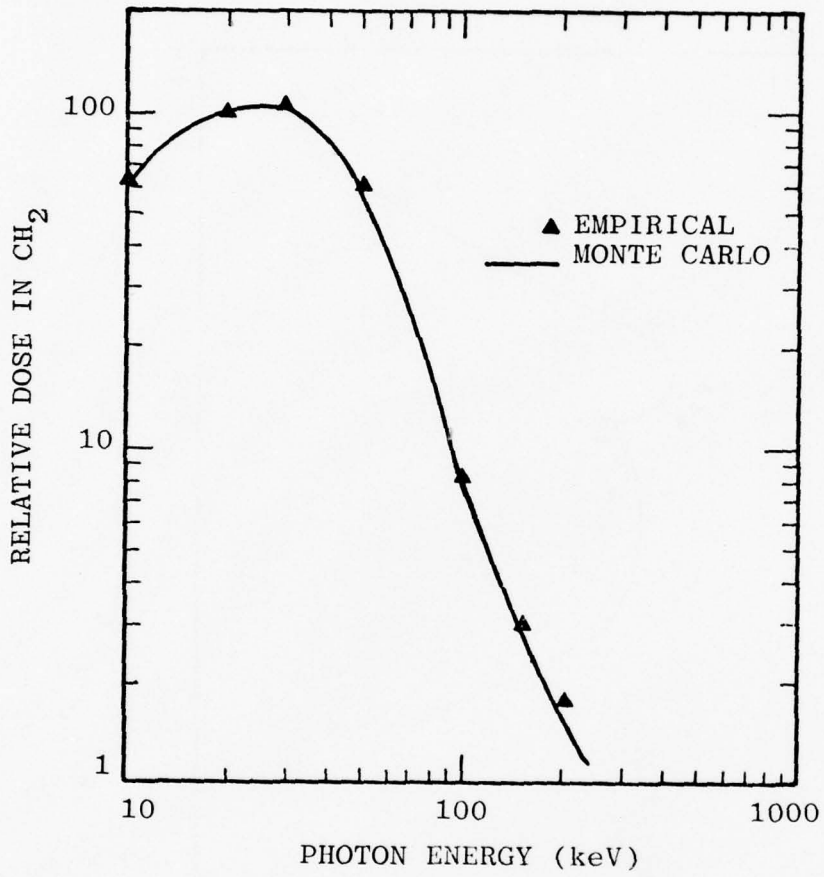

FIGURE 3. Comparison of Empirical Calculation With Monte Carlo Calculation: Relative Dose in Polyethylene at Copper Interface.

where D_{ro} is the interface dose obtained from equation (13) and a_i is the fractional contribution to the equilibrium dose in material 1 due to electrons produced in the i-th electron production interaction:

$$a_i = \frac{n_i \mu_i(h\nu) E_i}{\sum_j n_j \mu_j(h\nu) E_j} \tag{17}$$

The coefficient b_i is given by the ratio of the interface dose to the interface fluence; Burke and Garth obtain

$$b_i = 2\frac{m+1}{m} \frac{1+\beta_2}{1-\beta_2} \frac{1}{R_2(E_i)} \tag{18}$$

where m is the coefficient in the power function approximation to the csda electron range in material 1

$$R_1(E_i) = K E_i^m \tag{19}$$

The coefficient m in equation (19) is a slowly varying function of atomic number, $m = 1.65 \pm 0.10$, so we may to good approximation express the coefficient b_i by

$$b_i = 3.21 \frac{1+\beta_2}{1-\beta_2} \frac{1}{R_2(E_i)} \tag{20}$$

Following Burke's procedure we use the empirical formula for the normal electron reflection coefficient in evaluating equation (20)

$$\beta = 0.186Z^{0.318} - 0.25 \qquad (21)$$

rather than the diffuse reflection coefficient equation (15). Note that equations (16, 17 and 20) are equivalent to the expressions developed by Burke and Garth[7] but are in a simpler form.

The a_i coefficients in equation (16) represent the relative magnitudes of the source contributions to the interface dose. Shown in Table 2 are expressions for the a_i coefficients. Shown in Table 3 are sample calculations of the a_i coefficients for electrons arising in gold for several photon energies. Note that just above the K-absorption edge, $h\nu$ = 85 and 100 keV that strong contributions to the interface dose arise from L-Auger and M-Auger electrons as well as K-photoelectrons, L-photoelectrons, and K-Auger electrons. Because of the short ranges of the low energy L-Auger and M-Auger electrons (less than about 1 μm in silicon), they contribute to the dose only very near the interface. Further from the interface the dose is dominated by the contributions of the higher energy photoelectrons. For photon energies much greater than the K-absorption edge, the dose profile is dominated by K-photoelectron and L-photoelectron contributions.

The exponential approximation to the dose profile in equation (16) is not extremely accurate (in fitting Monte Carlo calculations of dose profiles we found it

---

[7] E. A. Burke and J. C. Garth, IEEE Trans. Nuc. Sci., NS-23, No. 6, 1838 (1976).

TABLE 2. a_i COEFFICIENTS

a_i COEFFICIENTS

$$a_K = \frac{\mu}{\mu_{en}} P_K \frac{h\nu - E_K}{h\nu}$$

$$a_L = \frac{\mu}{\mu_{en}} P_{\overline{L}} \frac{h\nu - E_{\overline{L}}}{h\nu}$$

$$a_M = \frac{\mu}{\mu_{en}} P_{\overline{M}} \frac{h\nu - E_{\overline{M}}}{h\nu}$$

$$a_{KA} = \frac{\mu}{\mu_{en}} P_K (1-W_K) \frac{E_K - 2E_{\overline{L}}}{h\nu}$$

$$a_{LA} = \frac{\mu}{\mu_{en}} (1-\omega_L) \left[P_{\overline{L}} + P_K(2-\omega_K) \right] \frac{E_{\overline{L}} - 2E_{\overline{M}}}{h\nu}$$

$$a_{MA} = \frac{\mu}{\mu_{en}} \left\{ P_{\overline{M}} + (2-\omega_L) \left[P_{\overline{L}} + P_K(2-\omega_K) \right] \right\} \frac{E_{\overline{M}}}{h\nu}$$

TABLE 2. a_i COEFFICIENTS (Continued)

MEAN BINDING ENERGIES

$$E_{\bar{L}} = \frac{1}{P_{\bar{L}}} (1-r_{L1})E_{L1}+r_{L1}(1-r_{L2})E_{L2}+r_{L1}r_{L2}(1-r_{L3})E_{L3}$$

$$E_{\bar{M}} = \frac{1}{P_{\bar{M}}} (1-r_{M1})E_{M1}+r_{M1}(1-r_{M2})E_{M2}+r_{M1}r_{M2}(1-r_{M3})E_{M3}$$

$$+r_{M1}r_{M2}r_{M3}(1-r_{M4})E_{M4}+r_{M1}r_{M2}r_{M3}r_{M4}(1-r_{M5})E_{M5}$$

PHOTOELECTRIC SHELL PROBABILITIES

$$P_K = 1 - r_K \qquad h\nu \geq E_K$$

$$= 0 \qquad h\nu < E_K$$

$$P_{\bar{L}} = r_K(1-r_{L1}r_{L2}r_{L3}) \qquad h\nu \geq E_K$$

$$= 1-r_{L1}r_{L2}r_{L3} \qquad E_{\bar{L}} \leq h\nu < E_K$$

$$= 0 \qquad h\nu < E_{\bar{L}}$$

TABLE 2. a_i COEFFICIENTS (Concluded)

PHOTOELECTRIC SHELL PROBABILITIES (Continued)

$$P_{\overline{M}} = r_K r_{L1} r_{L2} r_{L3} \qquad h\nu \geq E_K$$

$$= r_{L1} r_{L2} r_{L3} \qquad E_{\overline{L}} \leq h\nu < E_K$$

$$= 1 \qquad E_{\overline{M}} \leq h\nu < E_{\overline{L}}$$

$$= 0 \qquad h\nu < E_{\overline{M}}$$

NOTES:

(1) $r_i = \frac{\mu(E_i - \delta)}{\mu(E_i + \delta)}$ is the ratio of the photoelectric cross-sections just below and just above the photoelectric absorption edge E_i.

(2) ω_i = fluorescent yield (i = K,L).

TABLE 3. CONTRIBUTIONS TO INTERFACE DOSE BY ELECTRONS ARISING IN GOLD

a_i (Gold)

hν	a_K	a_L	a_M	a_{KA}	a_{LA}	a_{MA}
30	—	0.49	0.28	—	0.05	0.18
85	0.11	0.36	0.14	0.07	0.16	0.16
100	0.34	0.29	0.10	0.05	0.11	0.11
150	0.58	0.22	0.08	0.02	0.05	0.05

SOURCE SYMBOLS: K - K-photoelectrons, L - L-photoelectrons, M - M-photoelctrons, KA - K-Auger electrons, LA - L-Auger electrons, MA - M-Auger electrons.

necessary to use expressions of the form $a \exp(bx+cx^2+dx^3)$ to obtain accurate fits[2]), but based on results obtained by Burke and Garth[7] and by Dellum and MacCallum[11] it appears that the model is quite adequate for estimating the dose profile. As a check we compare the predictions of the simple model with POEM Monte Carlo calculations of the relative dose profile in silicon near gold for 100 keV photons in Figure 4, the agreement is seen to be good.

The empirical model assumes an isotropic distribution for the electron fluence in the bulk regions of the materials. This is a good approximation for photoelectrons and Auger electrons, but a poor approximation for Compton electrons. The model is thus limited to x-ray spectra for which the photon interaction cross section is dominated by the photoelectric effect; for high-Z/low-Z interfaces this limits the model to photon energies $h\nu \lesssim 400$ keV. This is the region in which the dose enhancement effect is greatest. For photon energies about this energy, a Monte Carlo calculation is probably required to obtain an accurate prediction of interface dose. Remember, though, that the maximum dose enhancement in this energy range is less than a factor of two.

The empirical model assumes equilibrium thicknesses for the high-Z and low-Z materials. The model is therefore limited to material thicknesses less than the maximum electron range; for thinner materials Monte Carlo calculations are

---

[2] W. L. Chadsey, J. C. Garth, R. L. Sheppard, and R. Murphy, "X-Ray Dose Enhancement," RADC Report TR-76-159 (1976).

[7] E. A. Burke and J. C. Garth, IEEE Trans. Nuc. Sci., NS-23, No. 6, 1838 (1976).

[11] T. A. Dellin and C. J. MacCallum, IEEE Trans. Nuc. Sci., NS-23, No. 6, 1844 (1976).

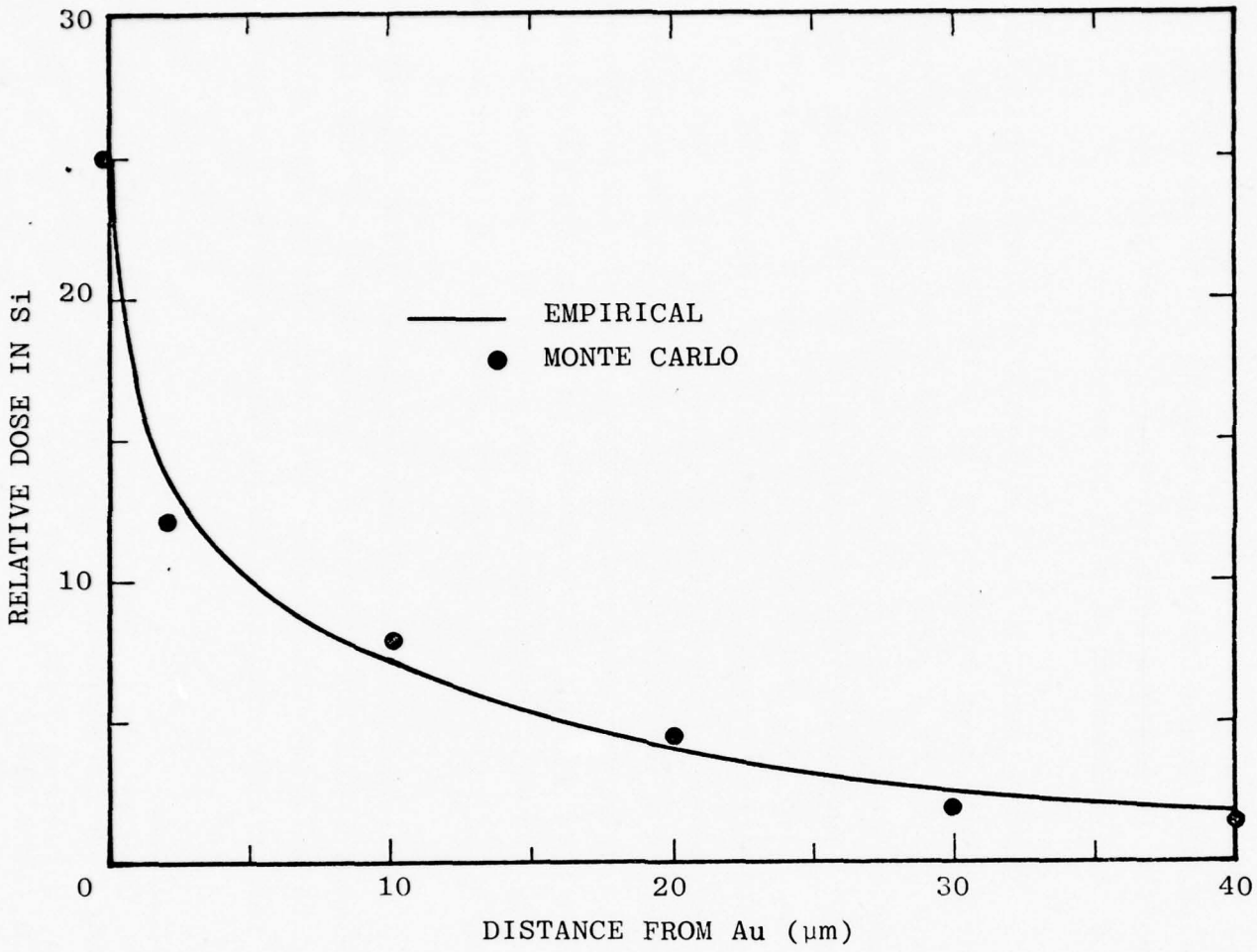

FIGURE 4. Comparison of Empirical Calculation with Monte Carlo Calculation: Relative Dose Profile in Silicon Near Gold, 100 keV X-Rays.

probably required. (In section 3 of this report we present Monte Carlo results for thin materials.)

2.3.3 Analytical Approximation

Dellin and MacCallum[11] have developed an analytical approximation for the prediction of the dose profile at an interface. The method is the extension of their earlier analytical approximations to the bulk photo-Compton current and vacuum emission current. A P_1 approximation to the Boltzman equation is solved to obtain the dose, energy fluence and charge fluence at the material interface. The dose profile is then calculated using the same exponential approximation as used in the empirical model discussed above.

This analytical approximation method was developed by Dellim and MacCallum into the QUICKE4 computer code. Calculations were performed and comparisons made with POEM and SANDYL Monte Carlo codes obtaining generally good agreement. To our knowledge the QUICKE4 computer code has not as yet been released to the community.

2.3.4 Monte Carlo Calculation

The most rigorous method of prediction of the dose enhancement is calculation with a Monte Carlo electron transport code. While Monte Carlo codes produce results subject to statistical uncertainty and are expensive in terms of computer time, the codes are exact from a physical standpoint and are applicable to arbitrary geometric and material

[11] T. A. Dellin and C. J. MacCallum, IEEE Trans. Nuc. Sci. NS-23, No. 6, 1844 (1976).

configurations. In particular, the Monte Carlo codes are applicable to the prediction of dose enhancement for cases of thin layers, multiple layers, or multiple dimensional configurations. Furthermore, the cost of a set of Monte Carlo calculations is small compared with the cost of developing an analytical prediction technique, and the Monte Carlo predictions can be used with high confidence based on extensive validation of the codes.

Monte Carlo codes calculate the transition zone dose in a two step process: (1) The electron source distribution in the neighborhood of the material interface is calculated, generally using an analytical formulation – the source distribution is comprised of photoelectrons, Auger electrons, Compton electrons, and for high photon energies electron-position pairs; (2) the electron transport is calculated in the neighborhood of the interface to obtain the energy deposition using a Monte Carlo formulation.

A number of available Monte Carlo electron transport codes are applicable to the calculation of dose enhancement. Most of these codes are decendents of the ETRAN code developed by Berger and Seltzer.[12] The two most commonly used codes are POEM[1] and SANDYL[13].

POEM is a special purpose, fast running Monte Carlo electron transport code with versions specifically

---

[1] W. L. Chadsey, "POEM," AFCRL Report TR-75-3034 (1975).

[12] M. J. Berger and S. M. Seltzer, "Electron and Photon Transport Programs," NBS Reports 9836-9837.

[13] H. M. Colbert, "SANDYL," Sandia Laboratories Report SLL-74-0012 (1974).

designed for the calculation of dose enhancement. There are two versions for this puppose: One for the calculation of the transition zone dose profile at a single planar interface between two materials; the other version calculates the dose profile in a stack of up to 20 slabs of materials. The materials may be any homogeneous material of a composition of up to ten elements. The elements may be any of those with atomic number Z = 1 through 83, 86, 90, 92 and 94. The photon spectrum can be (1) monochromatic, (2) blackbody spectrum, or (3) arbitrary spectrum defined over up to 120 photon energy groups. The photon spectral range of applicability of the code is approximately 5 keV through 2 meV. The lower limit is imposed by the 1 keV cutoff on the electron transport. The upper limit is imposed by the exclusion of pair production in the electron source calculation. The code assumes plane wave photon irradiation. The angle of incidence is arbitrary.

While the POEM code versions for the calculation of dose enhancement are one-dimensional, i.e. they treat slab geometry configurations, this limitation is generally not serious. So long as the minimum radius of curvature of the material inteface and the lateral dimensions of the configurations are large compared with the maximum electron range, then a configuration can be accurately represented as one-dimensional in the transport calculation.

By developing versions of the POEM code specifically designed for the calculation of dose enhancement, it was possible to obtain a high level of optimization and incorporate several variance reduction techniques. Consequently, POEM is a fast running Monte Carlo code. Our experience shows POEM to be about a factor of 20 faster

than general purpose Monte Carlo codes such as SANDYL. A typical calculation using 10,000 electron histories to obtain a 5 percent statistical error requires about 15 CPU seconds execution time on a CDC 7600 computer.

The POEM code calculations of dose enhancement we believe to be accurate to within about 25 percent. This is based on limited comparisons with experimental data for dose enhancement[5] and more extensive comparisons for x-ray photoemission.[4] Inter-code comparisons are also useful here: Published comparisons of SANDYL calculations with POEM calculations show agreement to within about 25 percent.[11]

The POEM code is available through the DASIAC code library (GE/TEMPO); in order to obtain the code written approval must be obtained from the Defense Nuclear Agency (DNA/RAEV). User's instructions for the POEM code are published in reference 1.

In order to obtain speed of computation, generality was necessarily sacrificed in developing the versions of POEM for predicting dose enhancement. If a dose enhancement problem requires a multidimensional calculation or prediction for photon energies much greater than 2 MeV, then a

---

[1] W. L. Chadsey, "POEM," AFCRL Report TR-75-2034 (1975).

[4] W. L. Chadsey and C. W. Wilson, "X-Ray Photoemission," HDL Report CR-75-138-1 (1975).

[5] W. L. Chadsey, "Monte Carlo Analysis of X-Ray and γ-Ray Transition Zone Dose and Photo-Compton Current," AFCRL Report TR-73-0572 (1973).

[11] T. A. Dellim and C. J. MacCallu, IEEE Trans. Nuc. Sci. NS-23, No. 6, 1844 (1976).

more general purpose Monte Carlo transport code is required. SANDYL is a general purpose code which is applicable to the calculation of dose for arbitrary three-dimensional configurations for photon energies from about 5 keV up through 10 GeV. The SANDYL code is available through the Sandia Corporation. User's instructions to the SANDYL cose are published in Reference 13.

---

[13] H. M. Colbert, "SANDYL," Sandia Laboratories Report SLL-74-0012 (1974).

Section 3

MONTE CARLO CALCULATIONS OF DOSE ENHANCEMENT

In a previous report on x-ray dose enhancement[2] we published results of Monte Carlo calculations of dose profiles in silicon near gold and in polyethylene near gold for photon energies in the range 10 keV to 2 meV. The gold/silicon interface was selected because of its occurance in electronic devices; the gold/polyethylene interface was selected because it represents a practical worst case. The calculations reported were limited to these two interface configurations; they were also limited to the cases of monochromatic photon spectra and thick gold layers. There is of course interest in other cases; below we investigate dose enhancement for other interface configurations, continuous x-ray spectra, and thin gold layers.

3.1 DOSE ENHANCEMENT AT METAL/POLYETHYLENE INTERFACES

Previously we reported calculations of dose enhancement in polyethylene (CH_2, effective $Z < 6$) near gold ($Z = 79$); this is a practical worst-case mismatch in atomic number; we therefore expect a practical worst-case dose enhancement for Au/CH_2. A convenient set of calculations to investigate the dose enhancement effect on atomic

---

[2] W. L. Chadsey, J. C. Garth, R. L. Sheppard, and R. Murphy, "X-Ray Dose Enhancement," RADC Report TR-76-159 (1976).

number are the interfaces Aℓ(Z=B)/CH_2, Cu(Z=29)/CH_2, Ag(Z=47)/CH_2, and Au/CH_2. These configurations are also of interest with regards to the analysis of radiation effects on cables. With respect to dose enhancement, polyethylene is representative of a broad class of low-Z dielectrics whereas the four metals represent aluminum, copper, and gold conductors and silvered (or tinned) copper conductors.

Interface dose enhancement in polyethylene versus photon energy is shown in Figure 5 for the four metals. Shown in Figures 6 through 9 are representative dose profiles for the four configurations.

3.2 DOSE ENHANCEMENT FOR CONTINUOUS X-RAY SPECTRA

The previously reported calculations were for cases of monochromatic photon spectra; this, of course, is the most convenient representation of spectra for characterizing dose enhancement versus photon energy. The radiation effects analyst, however, frequently represents continuous x-ray spectra with the Planckian (blackbody) distribution function. Shown in Figure 10 is the interface dose enhancement in silicon near gold versus x-ray spectrum blackbody temperature for the configuration shown. The incident spectrum is attenuated through 20 mils (0.0508 cm) of aluminum. The gold thickness is the equilibrium thickness. Results are shown for both photon incidence normal to the interface through the gold (the worst-case angle of incidence) and photon incidence normal to the interface through the silicon (the least worst-case angle of incidence). Note that the worst-case dose enhancement varies by less than a factor of two over the spectral temperature range 2 keV to 15 keV; the interface dose enhancement is 10 $\pm$ 50%. Representative dose profiles are shown in Figure 11.

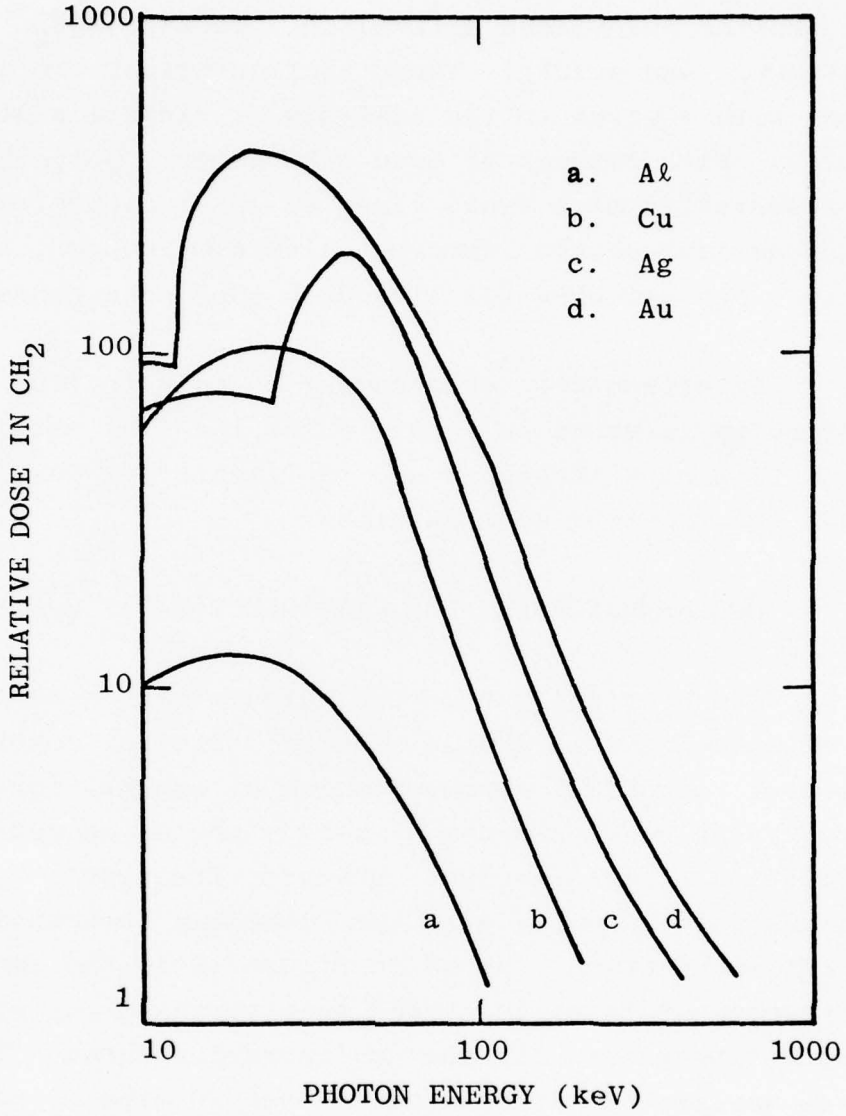

FIGURE 5. POEM Code Calculations of Relative Interface Dose in Polyethylene for Four Interface Metals: Aluminum, Copper, Silver, and Gold.

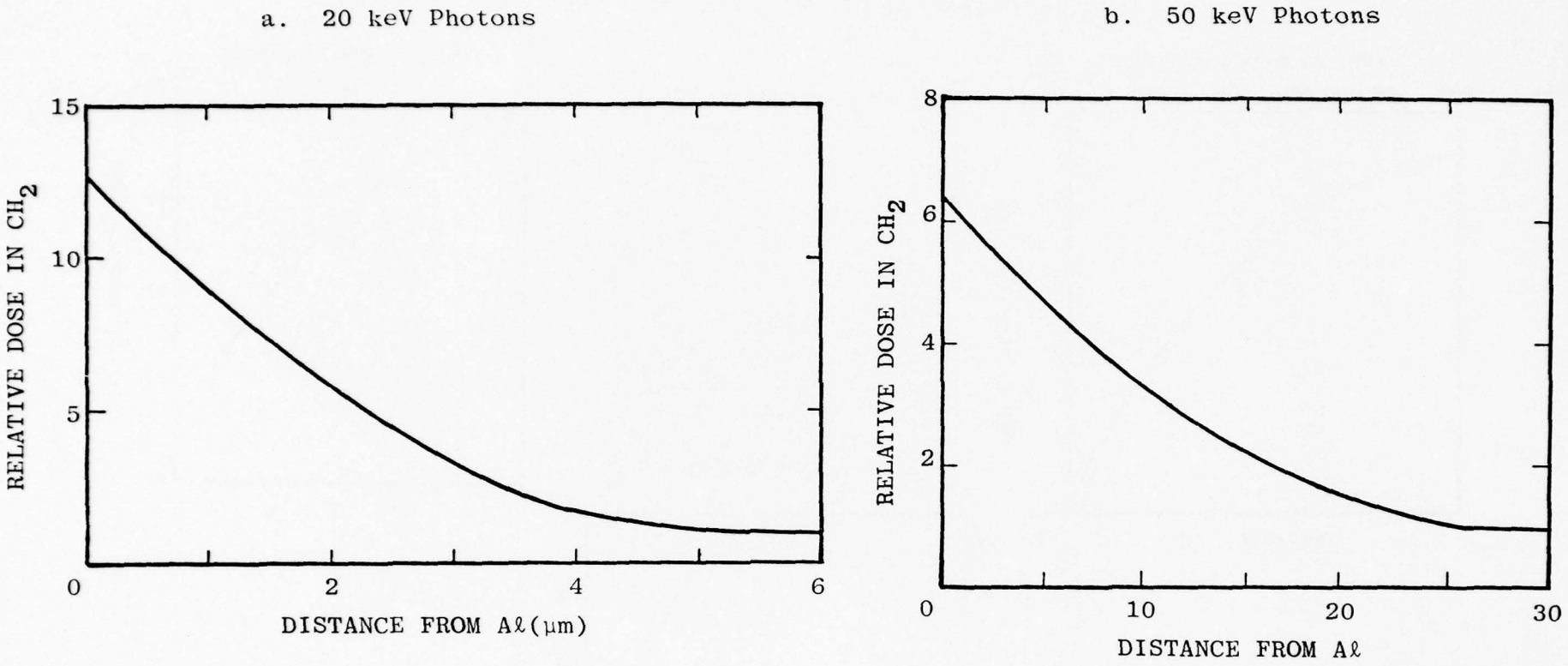

FIGURE 6. Relative Dose Profile in Polyethylene Near Aluminum: 20 keV and 50 keV Photons.

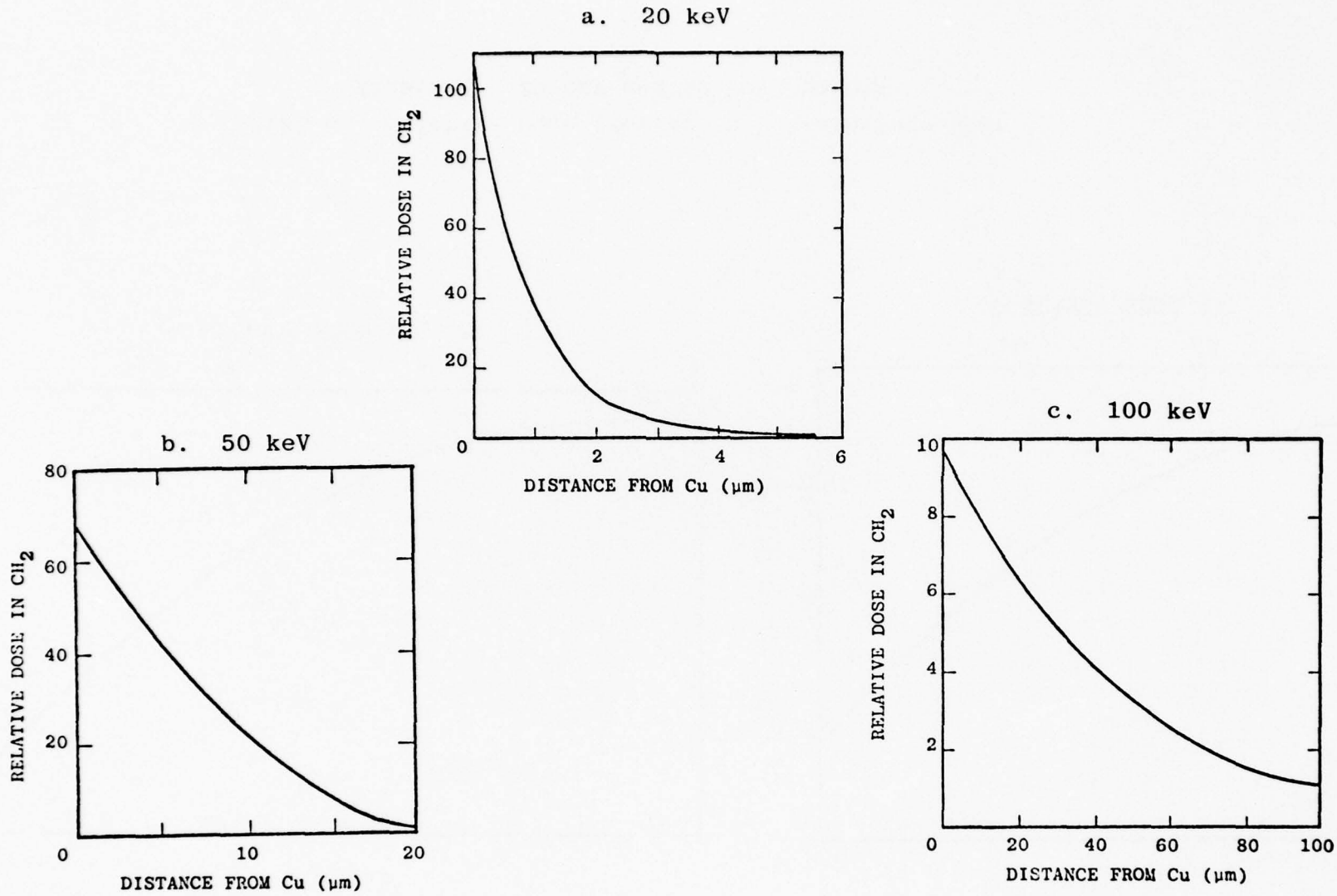

FIGURE 7. Relative Dose Profiles in Polyethylene Near Copper: 20, 50, and 100 keV Photons

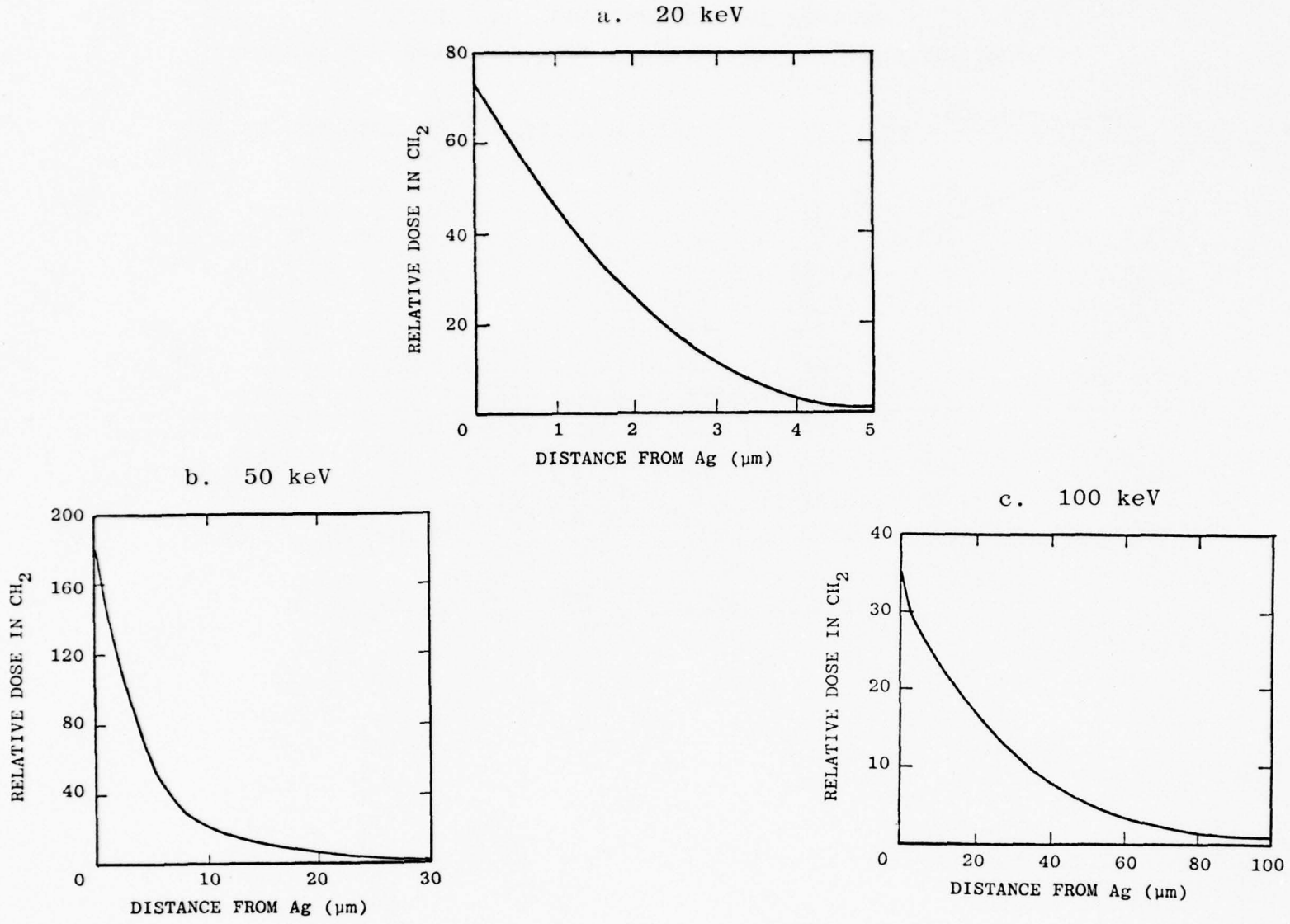

FIGURE 8. Relative Dose Profiles in Polyethylene Near Silver: 20, 50, and 100 keV Photons.

a. 20 keV

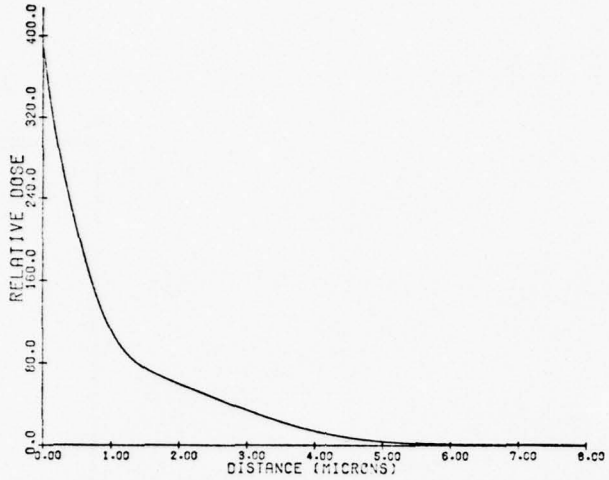

b. 50 keV

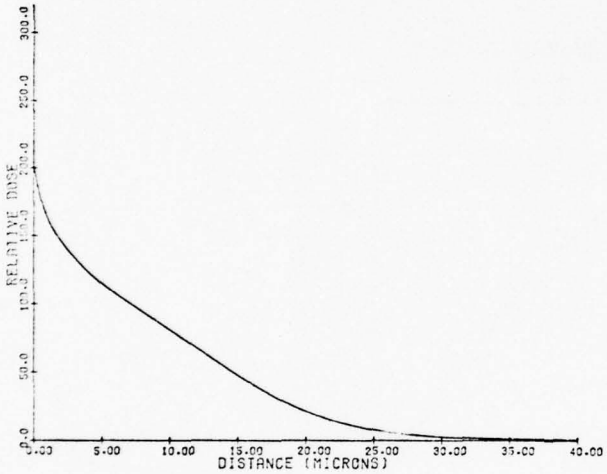

c. 100 keV

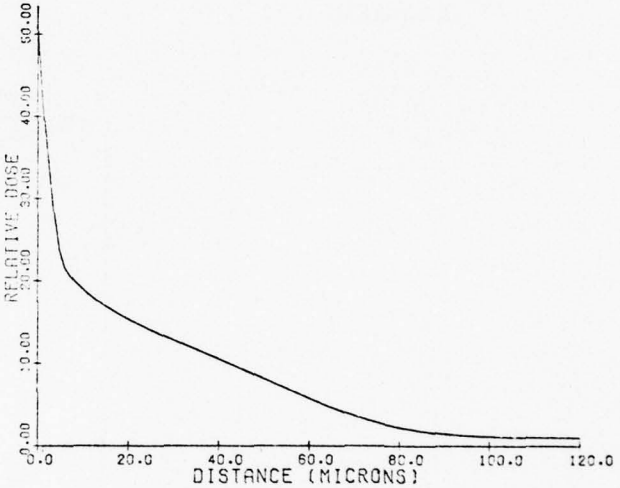

FIGURE 9. Relative Dose Profiles in Polyethylene Near Gold: 20, 50, and 100 keV Photons.

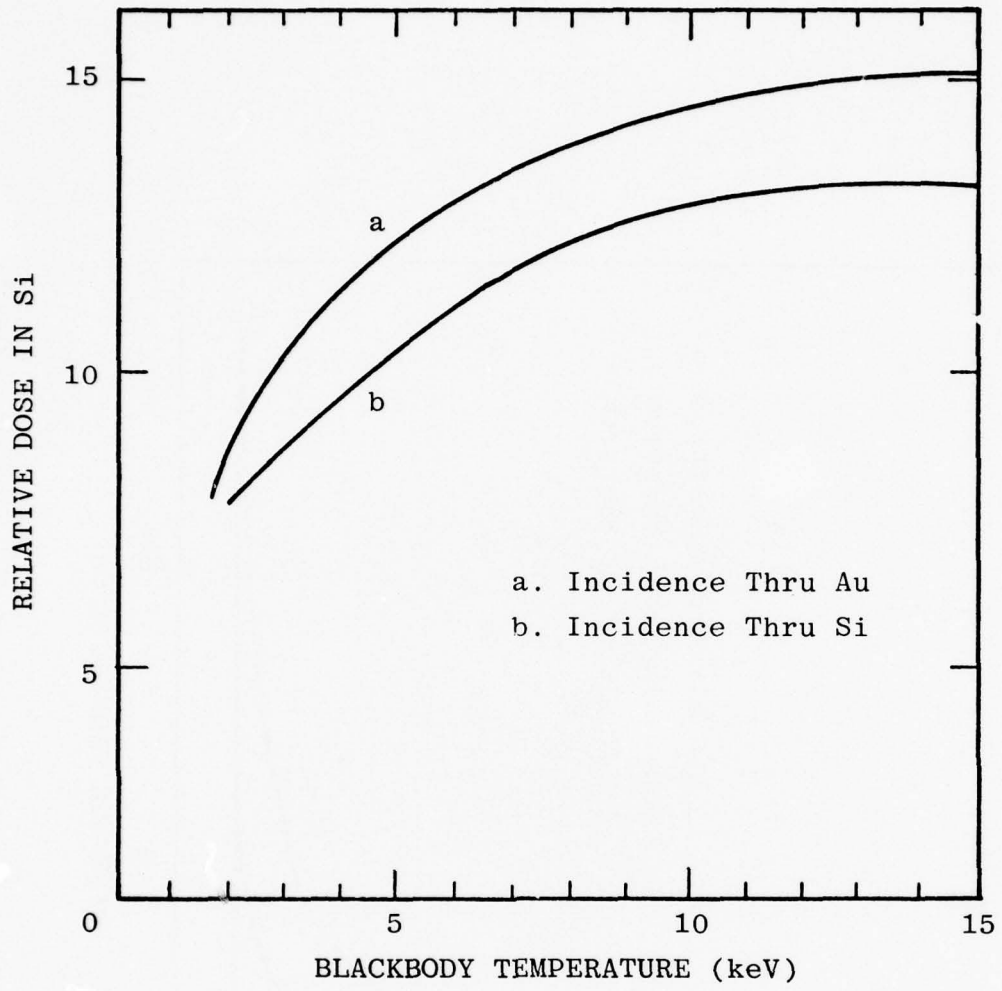

FIGURE 10. Relative Dose in Silicon at Gold Interface: Irradiation with Blackbody X-Ray Spectra Attenuated Through 20 Mils Aluminum.

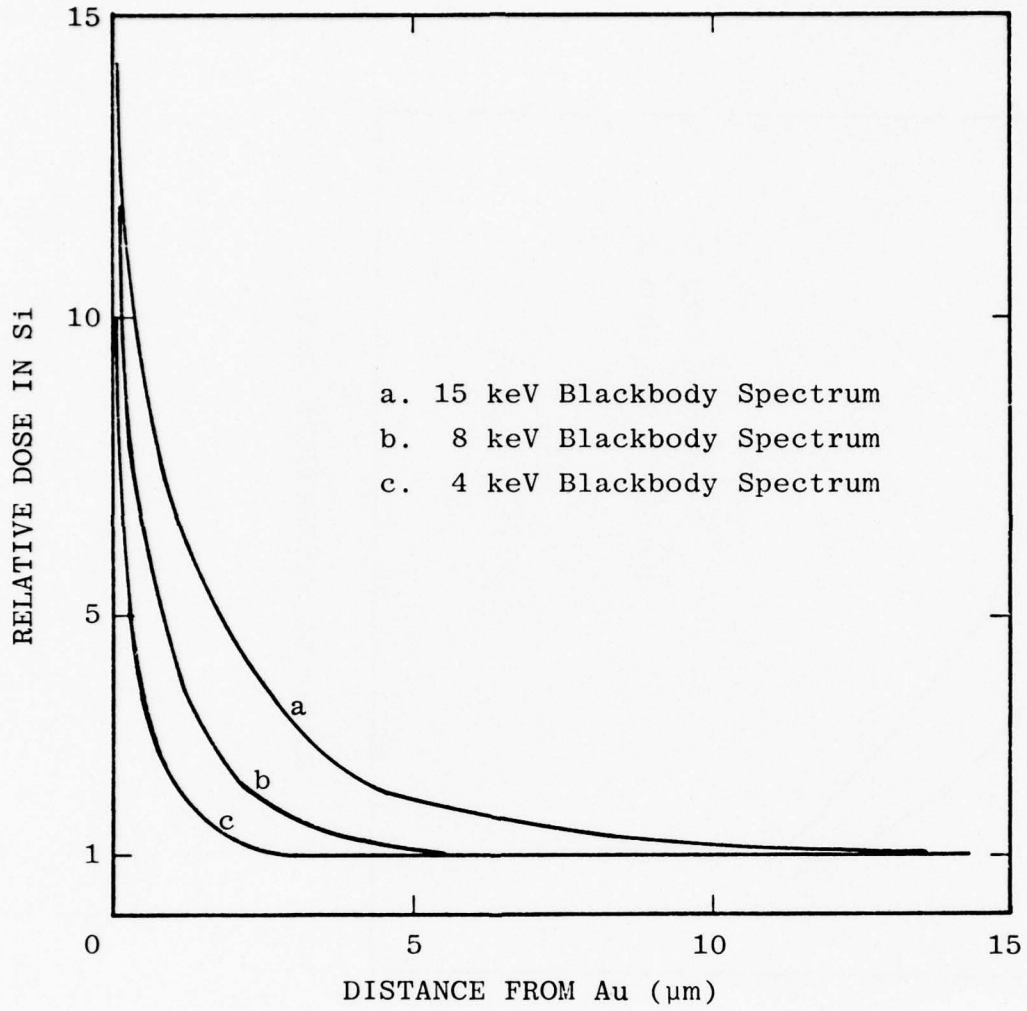

FIGURE 11. Relative Dose Profiles in Silicon Near Gold:
4, 8, and 15 keV Blackbody X-Ray Spectra Attenuated Through 20 Mils Aluminum.

3.3 DOSE ENHANCEMENT FOR THIN GOLD LAYERS

The dose enhancement calculations presented above and reported previously were all performed for thick gold layers. "Thick" here means thickness greater than or equal to the maximum electron range in gold. While this thickness is small (less than 15 μm for photon energies less than 100 keV), gold metalization thicknesses in electronic devices are often smaller than the equilibrium thickness. It is important therefore to characterize dose enhancement versus gold thickness. Shown in Figure 12 is the calculated dose enhancement in silicon near gold for gold thicknesses varying from zero to 80 μ-inches. The incident spectrum is a continuous x-ray spectrum with a mean energy of 55 keV. The equilibrium gold thickness for this spectrum is 14 μm (550 μ-inches); the dose enhancement for the equilibrium thickness is 19. Note that the dose enhancement is greater than 15 for gold layers as thin as 1 μm (40 μ-inches) which is less than one-tenth of the equilibrium thickness. This is because the mean electron penetration in gold is less than 10 percent of the csda range at these electron energies. The dose profiles in silicon are shown in Figure 13 for several gold layer thicknesses.

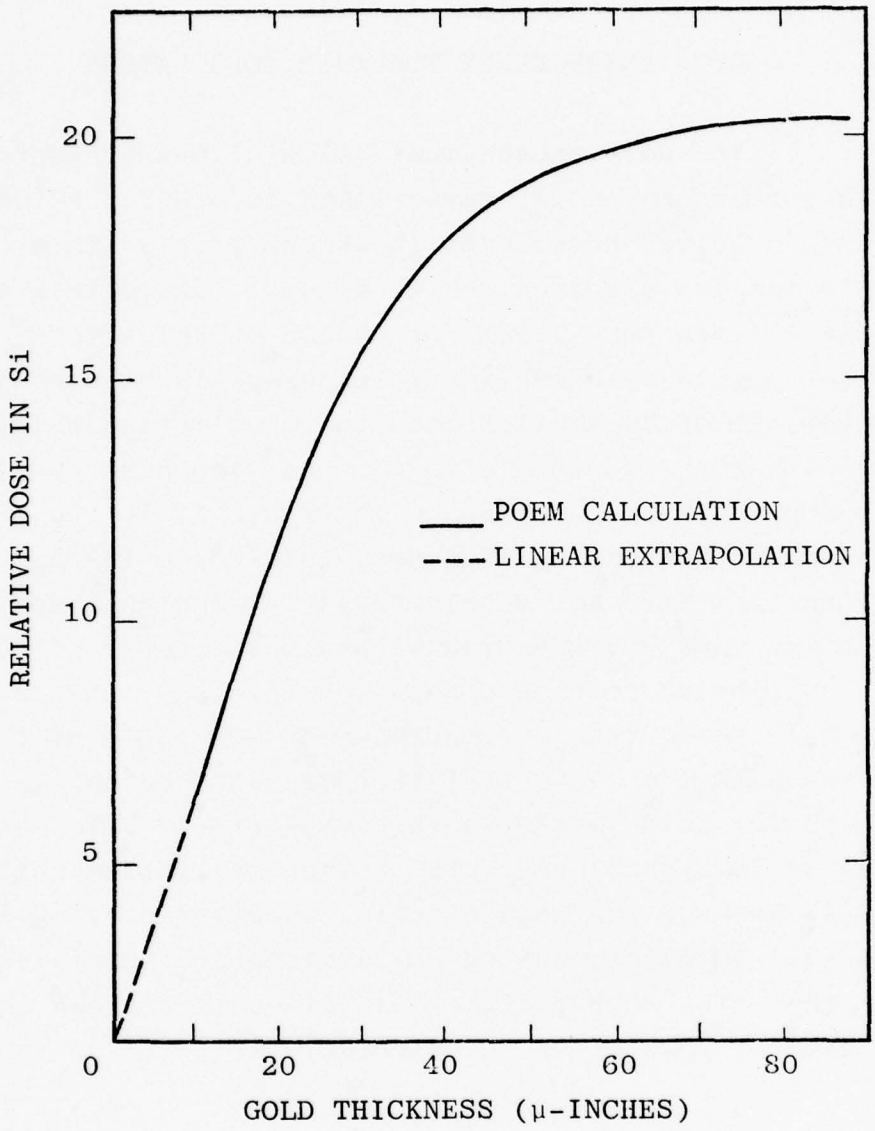

FIGURE 12. Dose Enhancement in Silicon at Gold Interface for Thin Gold Layer: Continuous X-Ray Spectrum with 55 keV Mean Energy.

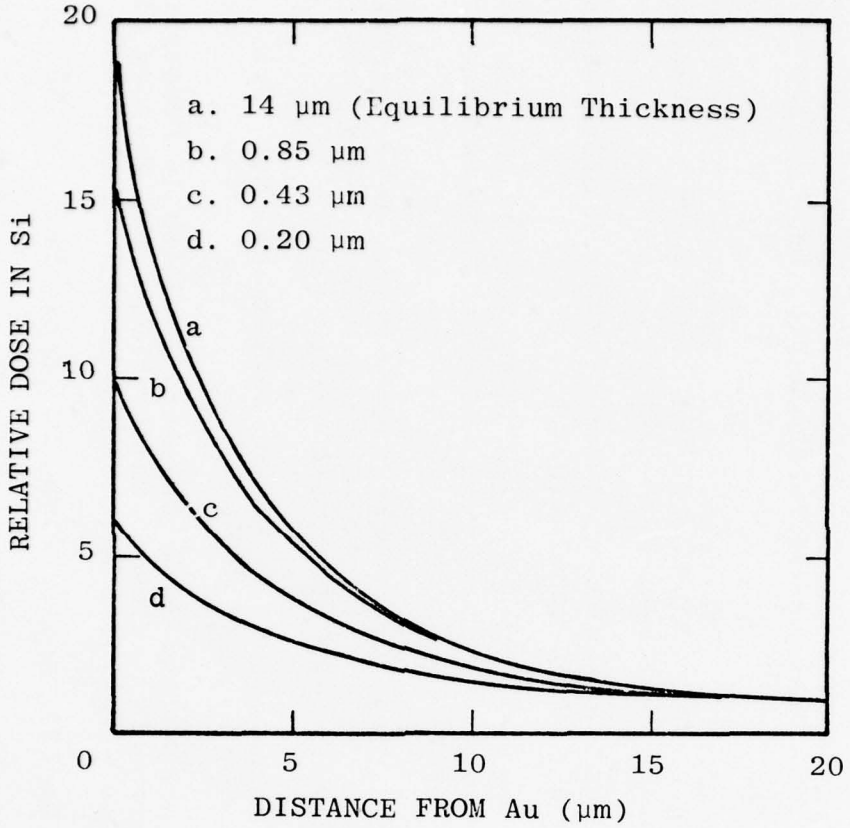

FIGURE 13. Dose Profiles in Silicon Near Gold: Thin Gold Layers; Irradiation with Continuous X-Ray Spectrum with 55 keV Mean Energy.

REFERENCES

1. W. L. Chadsey, "POEM," AFCRL Report TR-75-2023 (1975).

2. W. L. Chadsey, J. C. Garth, R. L. Sheppard, and R. Murphy, "X-Ray Dose Enhancement," RADC Report TR-76-159 (1976).

3. For example, E. Storm and H. I. Israel, "Photon Cross Sections from 0.001 to 100 MeV for Elements 1 through 100," LASL Report LA-2753 (1967).

4. W. L. Chadsey and C. W. Wilson, "X-Ray Photoemission," HDL Report CR-75-138-1 (1975).

5. W. L. Chadsey, "Monte Carlo Analysis of X-Ray and γ-Ray Transition Zone Dose and Photo-Compton Current," AFCRL Report TR-73-0572 (1973).

6. W. L. Chadsey, B. L. Beers, V. W. Pine, D. J. Strickland and C. W. Wilson, "X-Ray Photoemission; X-Ray Dose Enhancement" RADC Report TR-77-253 (1977).

7. E. A. Burke and J. C. Garth, IEEE Trans. Nuc. Sci., NS-23, No. 6, 1838 (1976).

8. M. J. Berger and S. M. Seltzer, "Studies in Penetration of Charged Particles in Matter," National Academy of Sciences - National Research Council Publ. No. 1133.

9. E. H. Darlington, J. Phys. D: Appl. Phys. 8, 85 (1975).

10. E. A. Burke, IEEE Trans. Nuc. Sci., NS-24, No. 6, 2505 (1977).

11. T. A. Dellin and C. J. MacCallum, IEEE Trans. Nuc. Sci., NS-23, No. 6, 1844 (1976).

12. M. J. Berger and S. M. Seltzer, "Electron and Photon Transport Programs," NBS Reports 9836-9837.

13. H. M. Colbert, "SANDYL," Sandia Laboratories Report SLL-74-0012 (1974).

DISTRIBUTION LIST

DEPARTMENT OF DEFENSE

Defense Communication Engineer Center
1860 Wiehle Ave
Reston, VA 22090
Attn: Code R320 C W Bergman
Attn: Code R410 J W McClean

Director
Defense Communications Agency
Washington, DC 20305
Attn: Code 540.5
Attn: Code 930 M I Burgett Jr

Defense Documentation Center
Cameron Station
Alexandria, VA 22314
Attn: TC

Director
Defense Intelligence Agency
Washington, DC 20301
Attn: DS-4A2

Director
Defense Nuclear Agency
Washington, DC 20305
Attn: TITL Tech Library
Attn: DDST
Attn: RAEV
Attn: STVL

Dir of Defense Rsch & Engineering
Department of Defense
Washington, DC 20301
Attn: S&SS (OS)

Commander
Field Command
Defense Nuclear Agency
Kirtland AFB, NM 87115
Attn: FCPR

Director
Interservice Nuclear Weapons School
Kirtland AFB, NM 87115
Attn: Document Control

Director
Joint Strat Tgt Planning Staff JCS
Offutt AFB Omaha, NB 68113
Attn: JLTW-2

Chief
Livermore Division Fld Command DNA
Lawrence Livermore Laboratory
P.O. Box 808
Livermore, CA 94550
Attn: FCPRL

Director
National Security Agency
Ft. George G. Meade, MD 20755
Attn: O O Van Gunten R-425
Attn: TDL

DEPARTMENT OF ARMY

Project Manager
Army Tactical Data Systems
US Army Electronics Command
Fort Monmouth, NJ 07703
Attn: DRCPN-TDS-SD
Attn: DWAINE B Huewe

Commander
BMD System Command
P.O. Box 1500
Huntsville, AL 35807
Attn: BDMSC-TEN

Commander
Frankford Arsenal
Bridge and Tacony Sts
Philadelphia, PA 19137
Attn: SARFA FCD

Commander
Harry Diamond Laboratories
2800 Powder Mill Road
Adelphi, MD 20783
Attn: DRXDO-EM
Attn: DRXDO-NP
Attn: DRXDO-TI/Tech Library
Attn: DRXDO-RB
Attn: DRXDO-RCC
Attn: DRXDO-RC
Attn: J Halpin
Attn: J McGarrity

Commanding Officer
Night Vision Laboratory
US Army Electronics Command
Fort Belvoir, VA 22060
Attn: Capt. Allan S Parker

Commander
Picatinny Arsenal
Dover, NJ 07801
Attn: SMUPA-FR-S-P
Attn: SARPA-FR-E
Attn: SMUPA-ND-W
Attn: SMUPA-ND-D-B
Attn: SARPA-ND-C-E
Attn: SARPA-ND-N
Attn: SMUPA-ND-N-E

Commander
Redstone Scientific Information Center
US Army Missile Command
Redstone Arsenal, AL 35809
Attn: Chief, Documents

Secretary of the Army
Washington, DC 20310
Attn: ODUSA or D Willard

Director
Trasana
White Sands Missile Range NM 88002
Attn: ATAA-EAC

Director
US Army Ballistic Research Labs
Aberdeen Proving Ground, MD 21005
Attn: DRXBR-X
Attn: DRXBR-VL
Attn: DRXBR-AM
Attn: DRXRD-BVL

Chief
US Army Communications Systems Agency
Fort Monmouth, NJ 07703
Attn: SCCM-AD-SV/Library

Commander
US Army Electronics Command
Fort Monmouth, NJ 07703
Attn: DRSEL-TL-IR
Attn: DRSEL-CE
Attn: DRSEL-CT-HDK
Attn: DRSEL-GG-TD
Attn: DRSEL-TL-MD
Attn: DRSEL-TL-ND
Attn: DRSEL-PL-ENV

Commandant
US Army Engineer School
Ft Belvoir VA 22060
Attn: ATSE-CTD-CS

Commander-in-Chief
US Army Europe & Seventh Army
APO New York 09403
(Heidelberg)
Attn: ODCSE-E AEAGE-PI

Commandant
US Army Field Artillery School
Fort Sill, OK 73503
Attn: ATSFA-CTD-ME

Commander
US Army Material Dev & Readiness CMD
5001 Esenhower Ave
Alexandria, VA 22333
Attn: DRCDE-D

Commander, US Army Missile Command
Redstone Arsenal, AL 35809
Attn: DRSI-RGP
Attn: DRCPM-PE-EA
Attn: DRSMI-RGD
Attn: DRSMI-RGP
Attn: DRSMI-RRR

Chief
US Army Nuc & Chemical Surety GP
Bldg 2073, North Area
Ft Belvoir, VA 22060
Attn: MOSG-ND

Commander
US Army Nuclear Agency
7500 Backlick Road
Building 2073
Springfield, VA 22150
Attn: ATCN-W

Commander
US Army Tank Automotive Command
Warren, MI 48090
Attn: DRCPM-GCM-SW

Commander
White Sands Missile Range
White Sands Missile Range NM 88002
Attn: STEWS-TE-NT

DEPARTMENT OF NAVY

Chief of Naval Research
Navy Department
Arlington, VA 22217
Attn: Code 427

Commander Officer
Naval Avionics Facility
21st & Arlington Ave
Indianapolis, IN 46218
Attn: Branch 942

Commander
Naval Electronic Systems Command Hqs
Washington, DC 20360
Attn: Code 504511
Attn: Code 50451
Attn: PME 117-21
Attn: Code 5032
Attn: Flex 05323

Commanding Officer
Naval Intelligence Support Ctr
4301 Suitland Road, Bldg. 5
Washington, DC 20390
Attn: NISC-45

Director
Naval Research Laboratory
Washington, DC 20375
Attn: Code 4004
Attn: Code 6631
Attn: Code 5210
Attn: Code 5216
Attn: Code 6460
Attn: Code 601
Attn: Code 7701
Attn: Code 2627

Commander
Naval Sea Systems Command
Navy Department
Washington, DC 20362
Attn: SEA-9931

Officer-in-Charge
Naval Surface Weapons Center
White Oak, Silver Spring, MD 20910
Attn: Code WA52
Attn: Code WA501/Navy Nuc Prgms Off
Attn: Code WA50

Commander
Naval Weapons Center
China Lake, CA 9355
Attn: Code 533 Tech Library

Commanding Officer
Naval Weapons Evaluation Facility
Kirtland AFB Albuquerque, NM 87117
Attn: Code ATG/Mr Stanley

Commanding Officer
Naval Weapons Support Center
Crane, IN 47522
Attn: Code 7024/J Ramsey
Attn: Code 70242/J A Munarin

Commanding Officer
Nuclear Weapons TNG Center Pacific
Naval Air Station, North Island
San Diego, CA 92135
Attn: Code 50

Director
Strategic Systems Project Office
Navy Department
Washington, DC 20376
Attn: SP 2701
Attn: NSP-2342
Attn: NSP-27331

DEPARTMENT OF THE AIR FORCE

RADC/Deputy for Electronic Technology
Hanscom AFB, MA 01731
Attn: ET/Stop 30/E Cormier
Attn: ES/Stop 30/F Shepherd
Attn: ES/Stop 30/E A Burke

AF Institute of Technology, AU
Wright-Patterson AFB, OH 45433
Attn: ENP/C J Bridgman

AF Materials Laboratory, AFSC
Wright-Patterson AFB, OH 45433
Attn: LTE

AF Weapons Laboratory, AFSC
Kirtland AFB, NM 87117
Attn: DES
Attn: ELA
Attn: ELP TREE SECTION
Attn: NT/Carl E Baum
Attn: ELS
Attn: NTS

AFTAC
Patrick AFB FL 32925
Attn: TFS/Maj M F Schneider

AF Avionics Laboratory, AFSC
Wright-Patterson AFB, OH 45433
Attn: DHE/H J Hennecke
Attn: DHM/C Friend
Attn: DH/Ltc McKenzie
Attn: AAT/M Friar

Commander
ASD
Wright-Patterson AFB, OH 45433
Attn: ASD/ENESS/P T Marth
Attn: ASD-YH-EX/Ltc R Leverette
Attn: ENACC/R L Fish

Hq ESD
Hanscom AFB, MA 01731
Attn: YSEV

Hq ESD
Hanscom AFB, MA 01731
Attn: YWET

Commander
Foreign Technology Division, AFSC
Wright-Patterson AFB, OH 45433
Attn: FTDP

Commander
Rome Air Development Center, AFSC
Griffiss AFB, NY 13440
Attn: RBRP
Attn: RBRAC

Commander
RADC/Deputy for Electronic Technology
Hanscom AFB, MA 01731
Attn: ES/A Kahan
Attn: ES/B Buchanan
Attn: ES/R Dolan

SAMSO/YE
Post Office Box 92960
Worldway Postal Center
Los Angeles, CA 90009
Attn: YEE

SAMSO/IN
Post Office Box 92960
Worldway Postal Center
Los Angeles, CA 90009
Attn: IND/I J Judy

SAMSO/MN
Norton AFB, CA 92409
Attn: MNNH

SAMSO/RS
Post Office Box 92960
Worldway Postal Center
Los Angeles, CA 90009
Attn: RSMG
Attn: RSSE

SAMSO/SK
Post Office Box 92960
Worldway Postal Center
Los Angeles, CA 90009
Attn: SKF

SAMSO/SZ
Post Office Box 92960
Worldway Postal Center
Los Angeles, CA 90009
Attn: SZJ

Commander in Chief
Strategic Air Command
Offutt AFB, NB 68113
Attn: XPFS
Attn: NRI-STINFO Library

US ENERGY RSCH & DEV ADMIN

University of California
Lawrence Livermore Laboratory
P. O. Box 808
Livermore, CA 94550
Attn: Hans Kruger L-96
Attn: Frederick R Kovar L-31
Attn: Donald J Meeker L-545
Attn: Tech Info Dept L-3
Attn: F K Miller L-156
Attn: William J Hogan L-531
Attn: Ronald L Ott L-531
Attn: Joseph E Keller Jr L-125
Attn: Lawrence Cleland L-156

Los Alamos Scientific Laboratory
P. O. Box 1663
Los Alamos NM 87545
Attn: Doc Con for B W Noel
Attn: Doc Con for J A Freed

SANDIA Laboratories
P. O. Box 5800
Albuquerque NM 87115
Attn: Doc Con for Org 2110/J A Hood
Attn: Doc Con for 3141 Sandia Rpt Coll
Attn: Doc Con for Org 2140/R Gregory

US Energy Research & Dev Admin
Albuquerque Operations Office
P. O. Box 5400
Albuquerque, NM 87115
Attn: Doc Con for WSSB

OTHER GOVERNMENT

Department of Commerce
National Bureau of Standards
Washington, DC 20234
Attn: Judson C French

DEPARTMENT OF DEFENSE
CONTRACTORS

Aerojet Electro-Systems Co.
Div of Aerojet-General Corp.
P. O. Box 296, 1100 W. Hollyvale Dr
Azusa, CA 91702
Attn: T D Hanscome

Aerospace Corp.
P. O. Box 92957
Los Angeles, CA 90009
Attn: John Ditre
Attn: Irving M Garfunkel
Attn: S P Bower
Attn: Julian Reinheimer
Attn: L W Aukerman
Attn: Library
Attn: William W Willis

Analog Technology Corp.
3410 East Foothill Boulevard
Pasadena, CA 91107
Attn: J J Baum

AVCO Research & Systems Group
201 Lowell St
Wilmington, MA 01887
Attn: Research Lib/A830 Rm 7201

EDM Corp.
7915 Jones Branch Drive
McClean, VA 22101
Attn: T H Neighbors

EDM Corporation
P. O. Box 9274
Albuquerque International
Albuquerque, NM 87119
Attn: D R Alexander

Bendix Corp.
Communication Division
East Joppa Road
Baltimore, MD 21204
Attn: Document Control

Bendix Corp.
Research Laboratories Division
Bendix Center
Southfield, MI 48075
Attn: Mgr Prgm Dev/D J Niehaus
Attn: Max Frank

Boeing Company
P. O. Box 3707
Seattle, WA 98124
Attn: H W Wicklein/MS 17-11
Attn: Itsu Amura/2R-00
Attn: Aerospace Library
Attn: R S Caldwell/2R-00
Attn: Carl Rosenberg/2R-00

Booz-Allen and Hamilton, Inc.
106 Apple Street
Tinton Falls, NJ 07724
Attn: Raymond J Chrisner

California Institute of Technology
Jet Propulsion Laboratory
4800 Oak Grove Drive
Pasadena, CA 91103
Attn: J Bryden
Attn: A G Stanley

Charles Stark Draper Laboratory Inc.
555 Technology Square
Cambridge, MA 02139
Attn: Kenneth Fertig
Attn: Paul R Kelly

Cincinnati Electronics Corp.
2630 Glendale - Milford Road
Cincinnati, OH 45241
Attn: Lois Hammond
Attn: C R Stump

Control Data Corporation
P. O. Box O
Minneapolis, MN 55440
Attn: Jack Meehan

Cutler-Hammer, Inc.
AIL Division
Comac Road
Deer Park, NY 11729
Attn: Central Tech Files/A Anthony

Dikewood Industries, Inc.
1009 Bradbury Drive, S. E.
Albuquerque, NM 87106
Attn: L Wayne Davis

E-Systems, Inc.
Greenville Division
P. O. Box 1056
Greenville, TX 75401
Attn: Library 8-50100

Effects Technology, Inc.
5383 Hollister Avenue
Santa Barbara, CA 93111
Attn: Edward J Steele

Exp & Math Physics Consultants
P. O. Box 66331
Los Angeles, CA 90066
Attn: Thomas M Jordan

Fairchild Camera & Instrument Corp.
464 Ellis St
Mountain View, CA 94040
Attn: Sec Dept for 2-233 D K Myers

Fairchild Industries, Inc.
Sherman Fairchild Technology Center
20301 Century Boulevard
Germantown, MD 20767
Attn: Mgr Config Data & Standards

Florida, University of
P. O. Box 284
Gainesville, FL 32601
Attn: Patricia B Rambo
Attn: D P Kennedy

Ford Aerospace & Communications Corp.
3939 Fabian Way
Palo Alto, CA 94303
Attn: Edward R Hahn/MS-X22
Attn: Donald R McMorrow/MS-G30
Attn: Samuel R Crawford/MS-531

Ford Aerospace & Comm Operations
Ford & Jamboree Roads
Newport Beach, CA 92663
Attn: F R Poncelet Jr.
Attn: Ken C Attinger
Attn: Tech Info Section

Franklin Institute, The
20th St and Parkway
Philadelphia, PA 19103
Attn: Ramie H Thompson

Garrett Corporation
P. O. Box 92248, 9851 Sepulveda Blvd
Los Angeles, CA 90009
Attn: Robert E Weir/Dept 93-9

General Dynamics Corp.
Electronics Div Orlando Operations
P. O. Box 2566
Orlando, FL 32802
Attn: D W Coleman

General Electric Company
Space Division
Valley Forge Space Center
Goddard Blvd King of Prussia
P. O. Box 8555
Philadelphia, PA 19101
Attn: Larry I Chasen
Attn: John L Andrews
Attn: Joseph C Peden/VFSC, Rm 4230M

General Electric Company
Re-Entry & Environmental Systems Div
P. O. Box 7722
3198 Chestnut St
Philadelphia, PA 19101
Attn: Robert V Benedict
Attn: John W Palchefsky Jr
Attn: Ray E Anderson

General Electric Company
Ordnance Systems
100 Plastics Ave.
Pittsfield, MA 01201

General Electric Company
Tempo-Center for Advanced Studies
816 State St (P O Drawer QQ)
Santa Barbara, CA 93102
Attn: Royden R Rutherford
Attn: DASIAC
Attn: M Espig
Attn: William McNamara

General Electric Company
Aircraft Engine Business Group
Evendale Plant Int Hwy 75 S
Cincinnati, OH 45215
Attn: John A Ellerhorst E2

General Electric Company
Aerospace Electronics Systems
French Road
Utica, NY 13503
Attn: Charles M Hewison/Drop 624
Attn: W J Patterson/Drop 233

General Electric Company
P. O. Box 5000
Binghamton, NY 13902
Attn: David W Pepin/Drop 160

General Electric Company-Tempo
c/o Defense Nuclear Agency
Washington, DC 20305
Attn: DASIAC
Attn: William Alfonte

General Research Corporation
P. O. Box 3587
Santa Barbara, CA 93105
Attn: Robert D Hill

Georgia Institute of Technology
Georgia Tech Research Institute
Atlanta, GA 30332
Attn: R Curry

Grumman Aerospace Corporation
South Oyster Bay Road
Bethpage, NY 11714
Attn: Jerry Rogers/Dept 533

GTE Sylvania, Inc.
Electronics Systems GRP-Eastern Div
77 A St
Needham, MA 02194
Attn: Charles A Thornhill, Librarian
Attn: James A Waldon
Attn: Leonard L Blaisdell

GTE Sylvania, Inc.
189 B St
Needham Heights, MA 02194
Attn: Paul B Fredrickson
Attn: Herbert A Ullman
Attn: H & V Group
Attn: Charles H Ramsbottom

Gulton Industries, Inc.
Engineered Magnetics Division
13041 Cerise Ave
Hawthorne, CA 90250
Attn: Engnmagnetics Div

Harris Corp.
Harris Semiconductor Division
P. O. Box 883
Melbourne, FL 32901
Attn: Wayne E Abare/MS 16-111
Attn: Carl F Davis/MS 17-220
Attn: T L Clark/MS 4040

Hazeltine Corp.
Pulaski Rd
Greenlawn, NY 11740
Attn: Tech Info Ctr/M Waite

Honeywell Inc.
Avionics Division
2600 Ridgeway Parkway
Minneapolis, MN 55413
Attn: Ronald R Johnson/A1622
Attn: R J Kell/MS S2572

Honeywell Inc.
Avionics Division
13350 US Highway 19 North
St Petersburg, FL 33733
Attn: H H Noble/MS 725-5A
Attn: S H Graaff/MS 725-J

Honeywell Inc.
Radiation Center
2 Forbes Road
Lexington, MA 02173
Attn: Technical Library

Hughes Aircraft Company
Centinela and Teale
Culver City, CA 90230
Attn: Dan Binder/MS 6-D147
Attn: Billy W Campbell/MS 6-E-110
Attn: Kenneth R Walker/MS D157
Attn: John B Singletary/MS 6-D133

Hughes Aircraft Co., El Segundo Site
P. O. Box 92919
Los Angeles, CA 90009
Attn: William W Scott/MS A1080
Attn: Edward C Smith/MS A620

IBM Corporation
Route 17C
Owego, NY 13827
Attn: Frank Frankovsky
Attn: Harry W Mathers/Dept M41

Intl Tel & Telegraph Corp
500 Washington Ave
Nutley, NY 07110
Attn: Alexander T Richardson

Ion Physics Corp.
South Bedford St
Burlington, MA 01803
Attn: Robert D Evans

IRT Corp.
P. O. Box 81087
San Diego, CA 92138
Attn: MDC
Attn: Leo D Cotter
Attn: R L Mertz

JAYCOR
205 S. Whitting St, Suite 500
Alexandria, VA 22304
Attn: Catherine Turesko
Attn: Robert Sullivan

Johns Hopkins University
Applied Physics Laboratory
Johns Hopkins Road
Laurel, MD 20810
Attn: Peter E Partridge

Kaman Sciences Corp.
P. O. Box 7463
Colorado Springs, CO 80933
Attn: Jerry I Lubell
Attn: Walter E Ware
Attn: John R Hoffman
Attn: Donald H Bryce
Attn: Albert P Bridges
Attn: W Foster Rich

Litton Systems, Inc.
Guidance & Control Systems Division
5500 Canoga Ave
Woodland Hills, CA 91364
Attn: John P Retzler
Attn: Val J Ashby/MS 67
Attn: R W Maughmer

Litton Systems, Inc.
Electron Tube Division
1035 Westminster Drive
Williamsport, PA 17701
Attn: Frank J McCarthy

Lockheed Missiles & Space Co. Inc.
P. O. Box 504
Sunnyvale, CA 94088
Attn: B T Kimura/Dept 81-14
Attn: E A Smith/Dept 85-85
Attn: George F Heath/Dept 81-14
Attn: Samuel I Taimuty/Dept 85-85
Attn: L Rossi/Dept 81-64

Lockheed Missiles & Space Co. Inc.
3251 Hanover St
Palo Alto, CA 94304
Attn: Tech Info Ctr D/Coll

M.I.T. Lincoln Laboratory
P. O. Box 73
Lexington, MA 02173
Attn: Leona Loughlin, Librarian A-082

Martin Marietta Aerospace
Orlando Division
P. O. Box 5837
Orlando, FL 32805
Attn: Jack M Ashford/MP-537
Attn: William W Mras/MP-413
Attn: Mona C Griffith/Lib MP-30

Martin Marietta Corp.
Denver Division
P. O. Box 179
Denver, CO 80201
Attn: Paul G Kase/Mail 8203
Attn: Research Lib 6617 J R McKee
Attn: J E Goodwin/Mail 0452
Attn: B T Graham/MS PO-454

McDonnel Douglas Corp.
P. O. Box 516
St Louis, MO 63166
Attn: Tom Ender
Attn: Technical Library

McDonnel Douglas Corp.
5301 Bolsa Ave
Huntington Beach, CA 92647
Attn: Stanley Schneider

McDonnel Douglas Corp.
3855 Lakewood Boulevard
Long Beach, CA 90846
Attn: Technical Library, C1-290/36-84

Mission Research Corp.
735 State St
Santa Barbara, CA 93101
Attn: William C Hart

Mission Research Corp.-San Diego
P. O. Box 1209
La Jolla, CA 92038
Attn: V A J Van Lint
Attn: J P Raymond

The MITRE Corp.
P. O. Box 208
Bedford, MA 01730
Attn: M E Fitzgerald
Attn: Library

National Academy of Sciences
2101 Constitution Ave, NW
Washington, DC 20418
Attn: National Materials Advisory Board
Attn: R S Shane, Nat Materials Advsy

University of New Mexico
Electrical Engineering & Computer
Science Dept
Albuquerque, NM 87131
Attn: Harold Southward

Northrop Corp.
Electronic Division
1 Research Park
Palos Verdes Peninsula, CA 90274
Attn: George H Towner
Attn: Boyce T Ahlport

Northrop Corp.
Northrop Research & Technology Ctr
3401 West Broadway
Hawthorne, CA 90250
Attn: Orlie L Curtis, Jr
Attn: David N Pocock
Attn: J R Srour

Northrop Corp.
Electronic Division
2301 West 120th St
Hawthorne, CA 90250
Attn: Vincent R DeMartino
Attn: Joseph D Russo
Attn: John M Reynolds

Palisades Inst for Rsch Services Inc.
201 Varick St
New York, NY 10014
Attn: Records Supervisor

Physics International Co.
2700 Merced St
San Leandro, CA 94577
Attn: Doc Con for C H Stallings
Attn: Doc Con for J H Huntington

R&D Associates
P. O. Box 9695
Marina Del Rey, CA 90291
Attn: S Clay Rogers

Raytheon Company
Hartwell Road
Bedford, MA 01730
Attn: Gajanan H Joshi, Radar Sys Lab

Raytheon Company
528 Boston Post Road
Sudbury, MA 01776
Attn: Harold L Flescher

RCA Corp.
Government Systems Division
Astro Electronics
P. O. 800, Locust Corner
East Windsor Township
Princeton, NJ 08540
Attn: George J Brucker

RCA Corporation
Camden Complex
Front & Cooper Sts
Camden, NJ 08012
Attn: E Van Keuren 13-5-2

Rensselaer Polytechnic Institute
P. O. Box 965
Troy, NY 12181
Attn: Ronald J Gutmann

Research Triangle Institute
P. O. Box 12194
Research Triangle Park, NC 27709
Attn: Eng Div Mayrant Simons Jr

Rockwell International Corp.
P. O. Box 3105
Anaheim, CA 92803
Attn: George C Messenger FB61
Attn: Donald J Stevens FA70
Attn: K F Hull
Attn: N J Rudie FA53
Attn: James E Bell, HA10

Rockwell International Corporation
3701 West Imperial Highway
Los Angeles, CA 90009
Attn: T B Yates

Rockwell International Corporation
Collins Divisions
400 Collins Road NE
Cedar Rapids, IA 52406
Attn: Dennis Sutherland
Attn: Alan A Langenfeld
Attn: Mildred A Blair

Sanders Associates, Inc.
95 Canal St
Nashua, NH 03060
Attn: Moe L Aitel NCA 1 3236

Science Applications, Inc.
P. O. Box 2351
La Jolla, CA 92038
Attn: J Robert Beyster

Science Applications, Inc.
Huntsville Division
2109 W Clinton Ave
Suite 700
Huntsville, AL 35805
Attn: Noel R Byrn

Singer Company (Data Systems)
150 Totowa Road
Wayne, NJ 07470
Attn: Tech Info Center

Sperry Flight Systems Division
Sperry Rand Corp.
P. O. Box 21111
Phoenix, AZ 85036
Attn: D Andrew Schow

Sperry Univac
Univac Park, P. O. Box 3535
St. Paul, MN 55165
Attn: James A Inda/MS 41T25

Stanford Research Institute
333 Ravenswood Ave
Menlo Park, CA 94025
Attn: Philip J Dolan
Attn: Arthur Lee Whitson

Stanford Research Institute
306 Wynn Drive, NW
Huntsville, AL 35805
Attn: MacPherson Morgan

Sundstrand Corp.
4751 Harrison Ave.
Rockford, IL 61101
Attn: Curtis B White

Systron-Donner Corp.
1090 San Miguel Road
Concord, CA 94518
Attn: Gordon B Dean
Attn: Harold D Morris

Texas Instruments, Inc.
P. O. Box 5474
Dallas, TX 75222
Attn: Donald J Manus/MS 72

Texas Tech University
P. O. Box 5404 North College Station
Lubbock, TX 79417
Attn: Travis L Simpson

TRW Defense & Space Sys Group
One Space Park
Redondo Beach, CA 90278
Attn: Robert M Webb R1 2410
Attn: Tech Info Center/S1930
Attn: O E Adams R1-2036
Attn: R K Plebuch R1-2078

TRW Defense & Space Sys Group
San Bernardino Operations
P. O. Box 1310
San Bernardino, CA 92402
Attn: R Kitter

United Technologies Corp.
Hamilton Standard Division
Bradley International Airport
Windsor Locks, CT 06069
Attn: Raymond G Giguere

Vought Corp.
P. O. Box 5907
Dallas, TX 75222
Attn: Technical Data Ctr

ADDITIONAL DISTRIBUTION LIST

Hanscom AFB, MA 01731
Attn: AFGL/SUSRP/Stop 30
Attn: AFGL/CC/Stop 30
Attn: AFGL/SUOL/Stop 20
Attn: ESD/XR/Stop 30
Attn: ESD/XR/Stop 30/D Brick
Attn: DCD/SATIN IV
Attn: MCAE/Lt Col D Sparks
Attn: ES/Stop 30
Attn: EE/Stop 30

Griffiss AFB, NY 13441
Attn: RADC/OC
Attn: RADC/IS
Attn: RADC/DC

Attn: RADC/IR
Attn: RADC/CA
Attn: RADC/TIR
Attn: RADC/DAP
Attn: RADC/TILD

Maxwell AFB, AL 36112
Attn: AUL/LSE-67-342

US Army Missile Command Labs
Redstone Scientific Information Ctr
Redstone Arsenal, AL 35809
Attn: Chief, Documents

SAMSO (YA/AT)
P. O. Box 92960
Worldway Postal Center
Los Angeles, CA 90009
Attn: Mr Hess

Naval Postgraduate School
Superintendent
Monterey, CA 93940
Attn: Library (Code 2124)

US Dept. of Commerce
Boulder Laboratories
Boulder, CO 80302
Attn: Library/NOAA/ERl

USAF Academy
Library
Colorado 80840
Attn: 80840

Eglin AFB, FL 32542
Attn: ADTC/DLOSL

Scott AFB, IL 62225
Attn: AWS/DNTI/Stop 400

NASA Scientific & Technical
Information Facility
P. O. Box 33
College Park, MD 20740

NASA Goddard Space Flight Center
Goddard Space Flight Center
Greenbelt, MD 20771
Attn: Technical Library, Code 252,
Bldg. 21

Naval Surface Weapons Center
White Oak Lab.
Silver Spring, MD 20910
Attn: Library Code 730, RM 1-321

US Naval Missile Center
Point Mugu, CA 93041
Attn: Tech. Library - Code N0322

NASA Johnson Space Center
Attn: JM6, Technical Library
Houston, TX 77058

NASA
Lewis Research Center
21000 Brookpark Road
Cleveland, OH 44135
Attn: Technical Library

Wright-Patterson AFB, OH 45433
Attn: AFAL/CA
Attn: AFIT/LD, Bldg. 640, Area B
Attn: ASD/ASFR
Attn: ASD/FTD/ETID

Defense Communications Engineering
Center
1860 Wiehls Ave
Reston, VA 22090
Attn: Code R103R

Director, Technical Information
DARPA
1400 Wilson Blvd.
Arlington, VA 22209

Department of the Navy
800 North Quincy St
Arlington, VA 22217
Attn: ONRL Documents, Code 102IP

SAMSO
P. O. Box 92960
Worldway Postal Center
Los Angeles, CA 90006
Attn: Lt Col Staubs

US Army Electronics Command
Fort Monmouth, NJ 07703
Attn: AMSEL-GG-TD

Kirtland AFB NM 87117
Attn: AFWL/SUL Technical Library

US Naval Weapons Center
China Lake, CA 93555
Attn: Technical Library

Los Alamos Scientific Lab.
P. O. Box 1663
Los Alamos, NM 87544
Attn: Report Library

Hq DNA
Washington DC 20305
Attn: Technical Library

Secretary of the Air Force
Washington DC 20330
Attn: SAFRD

Scott AFB IL 62225
Attn: ETAC/CB/Stop 825

Andrews AFB
Washington DC 20334
Attn: AFSC/DLC

Army Material Command
Washington, DC 20315
Attn: AMCRD

NASA Langley Research Center
Langley Station
Hampton, VA 23365
Attn: Technical Library/MS 185

NASA
Washington DC 20546
Attn: Library (KSA-10)

Andrews AFB
Washington, DC 20334
Attn: AFSC/DLS

AFOSR, Bldg 410
Bolling AFB, Washington DC 20332
Attn: CC

AFML
Wright Patterson AFB, OH 45433

The Pentagon
Room 3-D-139
Washington, DC 20301
Attn: ODDR&E-OSD (Library)

ONR (Library)
Washington, DC 20360

Defense Intelligence Agency
Washington, DC 20301
Attn: SO-3A

AFAL
Wright-Patterson AFB, OH 45433
Attn: WRA-1/Library
Attn: TSR-5/Technical Library

Advisory Group on Electron Devices
201 Varick St, 9th Floor
New York, NY 10014

White Sands Missile Range, NM 88002
Attn: STEWS-AD-L/Technical Library

University of New Mexico
Dept of Campus Security & Police
1821 Roma, NE
Albuquerque, NM 87106
Attn: D Neaman

Health and Safety Division
Oak Ridge National Laboratory
P.O. Box X
Oak Ridge Tenn. 37830
Attn: Dr. J. Ashley

AFWL/DYC/Frank P. Cassisa
Kirtland AFB Albuquerque NM 87117

RADC/ESR/Stop 30/C. A. McCartney
Hanscom AFB MA 01731

MISSION
of
Rome Air Development Center

RADC plans and conducts research, exploratory and advanced development programs in command, control, and communications (C^3) activities, and in the C^3 areas of information sciences and intelligence. The principal technical mission areas are communications, electromagnetic guidance and control, surveillance of ground and aerospace objects, intelligence data collection and handling, information system technology, ionospheric propagation, solid state sciences, microwave physics and electronic reliability, maintainability and compatibility.

Printed by
United States Air Force
Hanscom AFB, Mass. 01731